

---

# CO2 Network

---

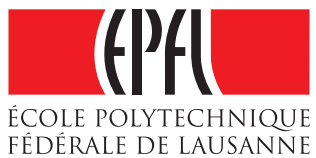
Case Study: ...

Tobia Wyss<sup>\*2</sup>, Luise Middelhauve<sup>†1</sup>, Luc Girardin<sup>‡1</sup>, and François Maréchal<sup>§1</sup>

<sup>1</sup>*Industrial Process and Energy Systems Engineering (IPESE), EPFL*

<sup>2</sup>*Master Student, Energy Management and Sustainability , EPFL*

January 28, 2019



---

<sup>\*</sup>tobia.wyss@epfl.ch

<sup>†</sup>luise.middelhauve@epfl.ch

<sup>‡</sup>luc.girardin@epfl.ch

<sup>§</sup>francois.marechal@epfl.ch



## Todo list

CO2den: necessary to talk about the advantage of expanding network with additional compressor easier than for water?? . . . . .	8
CO2den: need more drawbacks? or write more about it? . . . . .	8
CO2gva: Talk about financial numbers comparison? Otherwise delete fig 8 . . . . .	8
where to put this section? . . . . .	9
Figure: graph Q(T) for DX-GSHP . . . . .	11
find cheatsheet of exam MOES to do that . . . . .	11
is third eq rtk+1 = 0 correct??? . . . . .	11
add this paragraph . . . . .	12
dtmin finish rewriting this last part . . . . .	14
cite anything, or name is enough? . . . . .	15
other names? . . . . .	15
how has this temperature been chosen? is there a paper? see henchoz with other T . . . . .	20
write section eglantine calculations/energy demand . . . . .	24
add images of gradient and surface temperature from PGG report? . . . . .	26
this cost function here? . . . . .	27
insert equations for temperatures with dTmins? . . . . .	28
Figure: add figure with load profile . . . . .	29
Figure: energy schema ref scenario . . . . .	31
Figure: energy syst schema CO2 DEN . . . . .	32
explain lake=ref, geoth=DHX CO2 . . . . .	33
summary table needed here (Ts, dTmin, Tevap, P...)? wrong values now . . . . .	34
Table with values . . . . .	34
missing reference for superheat and subcool temp . . . . .	34
not sure where to put that... . . . . .	36
do i maintain results with simple cycles somewhere in the results to show how much better it is with cycle? . . . . .	37
write and reference model with if conditions . . . . .	44
wrapfig . . . . .	44
good thing to do? . . . . .	45
exergy and cop values . . . . .	45
needed figure of source? . . . . .	46
wrapfig . . . . .	47

### **Abstract**

District energy systems present a high potential to reduce CO<sub>2</sub> emissions caused by cities, thanks to the implementation of large polygeneration energy conversion technologies connected to buildings over a network. A specific technology, developed by EPFL, using a CO<sub>2</sub> network... A comparative analysis shows that...

# Contents

<b>1</b>	<b>Introduction</b>	<b>2</b>
1.1	Context . . . . .	2
1.2	Scope . . . . .	3
<b>2</b>	<b>State of the art</b>	<b>3</b>
2.1	District heating . . . . .	3
2.2	Fifth generation district energy networks . . . . .	4
2.3	CO <sub>2</sub> DEN . . . . .	6
2.3.1	The technology . . . . .	6
2.3.2	Performance . . . . .	8
2.3.3	Integration in smart energy system . . . . .	8
2.4	Direct-expansion ground source heat pump . . . . .	9
2.5	optimization . . . . .	11
2.5.1	MILP . . . . .	11
2.6	Osmose . . . . .	11
<b>3</b>	<b>Methodology</b>	<b>12</b>
3.1	Energy demand / Typical days . . . . .	12
3.2	Geothermal wells . . . . .	13
3.3	Investment cost function . . . . .	13
3.4	Minimum approach temperature . . . . .	14
3.5	Exergy . . . . .	15
3.6	Energy technology models . . . . .	15
3.6.1	Heat pumps - basic (Carnot) . . . . .	16
3.6.2	Heat pumps - detailed (Thermodyn.) . . . . .	16
3.6.3	Heat pump - supercritical CO <sub>2</sub> . . . . .	18
3.6.4	Cooling tower / Air cooler . . . . .	19
3.6.5	Geo-cooling . . . . .	20
3.6.6	PV . . . . .	20
3.6.7	Network . . . . .	20
<b>4</b>	<b>Application</b>	<b>21</b>
4.1	Case-study Eglantine . . . . .	21
4.1.1	Context . . . . .	21
4.1.2	Buildings . . . . .	22
4.1.3	Pre-studies . . . . .	22
4.1.4	Calculations/Energy demand/Typical days . . . . .	24
4.2	Heat sources . . . . .	25
4.2.1	Stream . . . . .	25
4.2.2	Lake . . . . .	25
4.2.3	Geothermal wells . . . . .	26
4.3	External heat sources . . . . .	27
4.3.1	Ice rink . . . . .	27
4.3.2	Shopping mall . . . . .	30
4.4	Variants / Scenarios . . . . .	30
4.4.1	Heating . . . . .	30
4.4.2	Cooling . . . . .	30
4.4.3	Refrigeration . . . . .	30
4.5	Reference scenario . . . . .	31
4.5.1	Heating . . . . .	31
4.5.2	Cooling . . . . .	32
4.5.3	Refrigeration . . . . .	32
4.6	CO <sub>2</sub> DEN . . . . .	32
4.6.1	Heating . . . . .	32
4.6.2	Refrigeration . . . . .	33

4.6.3	Cooling . . . . .	33
4.6.4	Central plant . . . . .	33
4.7	Values/typical days/... . . . . .	34
4.7.1	Investment cost functions . . . . .	34
4.7.2	Minimum approach temperature . . . . .	35
4.7.3	Compressor efficiencies . . . . .	35
4.8	CP with if conditions . . . . .	36
4.9	DX Vs. SL-GSHP . . . . .	36
4.10	Model improvement - thermodyn cycle . . . . .	37
<b>5</b>	<b>Results and discussion</b>	<b>38</b>
5.1	Energy and exergy performance . . . . .	38
5.2	Financial analysis . . . . .	40
5.2.1	Reference energy system . . . . .	41
5.2.2	CO2 DEN on geothermal wells . . . . .	42
5.3	Ground temperature . . . . .	43
5.4	Lake distance . . . . .	44
5.5	External heat source . . . . .	45
5.6	Optimization of energy demand . . . . .	45
5.6.1	Ground/CU . . . . .	48
<b>6</b>	<b>Outlook</b>	<b>48</b>
<b>7</b>	<b>Conclusion</b>	<b>49</b>
<b>8</b>	<b>Anergy nets Switzerland</b>	<b>51</b>

# Glossary

SH DHW REF AC GC CP ERA PV HP GSHP SL- DX- SIA PV DEN HEX DH DHC CHP is mech comp ex evap cond MILP PtG DSM HFC HCFC CFC HFO IC OC TC CAPEX OPEX

## 1 Introduction

### 1.1 Context

Throughout the last decades, human society has developed thanks to energy, most of which has come from fossil fuels. This has led to an unprecedented rise in CO<sub>2</sub> emissions, which have proved to be at the source of climate change. In order to secure a livable planet for the years to come, it is necessary, among others, to drastically reduce CO<sub>2</sub> emissions[?]. Since the adoption of the Kyoto protocol, the first international treaty about the fight against climate change in 1992, many countries have agreed to drastically reduce CO<sub>2</sub> emissions in the coming decades.

One crucial sector is the production of heat, which represents a large share of the total greenhouse emissions. This is especially true for countries at higher latitudes, i.e. with cold climates. For example in Switzerland the energy demand for space heating and hot water demand of buildings, accounts for around 41% (96.5 TWh) of the total energy demand of the country, and is still strongly dependent from fossil fuels. If we also include process heat, this figure rises to 54% (123.9 TWh)[?].

Also the energy demand related to cooling is experiencing an exponential growth. This is, on the one hand, because it is becoming affordable for more people, as income levels rise. On the other hand, this increase is due to global warming, which leads worldwide to a higher average temperature, as well as an increase in the frequency of days with extreme temperatures[?]. There are today 1.6 billion air conditioners (AC) in use, and about 50% of them are distributed in only two countries: China and USA. In some countries, especially in the Middle East, as well as in parts of the USA, during extremely hot days cooling can represent more than 70% of peak residential electricity demand. A huge problem with respect to this, is the quality of ACs. The majority of ACs that are sold in large markets, have an efficiency, which is only 50% or lower than the one of the best products available. This engenders, obviously, an important augmentation of the energy demand. Figure 1 shows how the energy demand has tripled since 1990, while the share of cooling energy in total energy use in buildings has risen from 2% to more almost 7% [?].

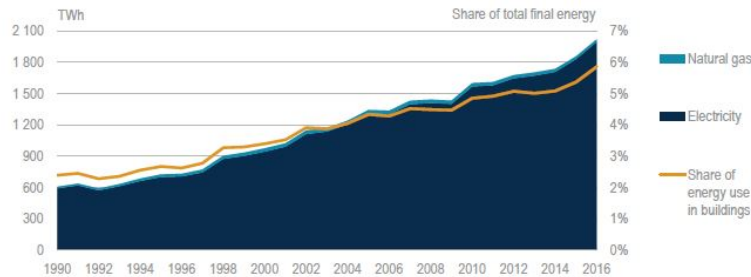


Figure 1: World energy consumption for space cooling in buildings. Source:[?]

A study shows that also in Switzerland cooling demand will strongly increase in the next decades, due to climate change. Figure 2 shows how this is particularly true for modern houses, which are very well isolated and efficient for the winter use. In this case the cooling demand will represent more or less a third of the heating demand[?].

According to the Population Division of the United Nations, the share of the world population living in cities has steadily increased from 34% in 1960 to 55% in 2017. Moreover, they prospect that, by 2050, this number will rise to 66%. In Switzerland, as well as in its neighbouring countries, the percentage of urban population is considerably higher, with 74% (2017) [?]. The fact that

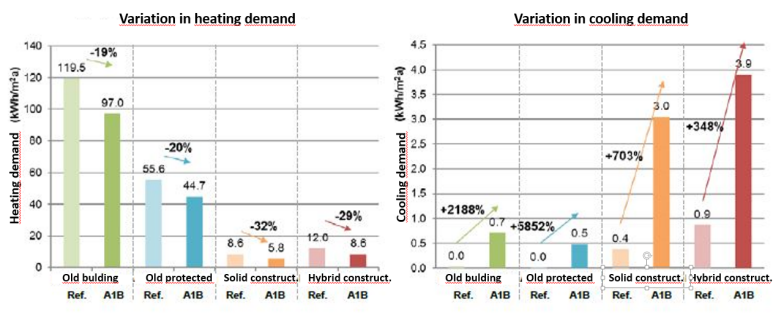


Figure 2: The evolution of median values of heating (left) and cooling (right) demand of the fours case studies ("Old building", "Old builing protected", "Solid construction", "Hybrid construction") between the reference period "1995" (1980-2009) and the period "2060" (2045-2074) in Basel. The percentage variations can be attributed to climate change. A1B corresponds to a median scenario developed by the IPCC. Source: [?]

people live more and more in concentrated areas, also mean that the density of energy consumption is rising. This becomes particularly interesting for urban heating and cooling demand, since the high density of heat consumers sets the conditions for efficient systems, based on district energy networks.

The UNEP (United Nations Environment Programme) has identified a big potential in modern district energy systems, as the most effective approach to improve energy efficiency for heating and cooling, and enable the integration of renewable energies. However, these technologies require a high level of technology coordination and planning, since they create more efficient systems that are also more complex to deploy and operate. This is why, further research and technology development are needed in order to foster the spreading of these technologies.

## 1.2 Scope

The scope of this project is to pursue the study of the application of the CO<sub>2</sub> based district energy network technology, proposed by Weber and Favrat[?]. In collaboration with Romande Energie, the utility company of canton Vaud, a feasibility study has to be performed on a specific case study: the residential district Eglantine in Morges. The work will try to answer the main research questions:

*How does the CO<sub>2</sub> district energy network perform - ecologically as well as financially - in the Eglantine district, and under which conditions does it perform better than concurrent solutions?*

*What are the characteristics of a typical district that favour the choice of the CO<sub>2</sub> district energy network technology?*

## 2 State of the art

### 2.1 District heating

The evolution of the technology of district heating (DH) is shown in Figure 3. The first District Heatings (DH) have been installed in the 1880s in the USA, using concrete ducts to distribute steam at high temperature, which was then condensed by the consumers. This system was obviously not very efficient, due to the elevated heat losses during transportation, as well as the exergy losses due to the high temperature level. In the early 1930 a second generation was developed, which based on the use of pressurized water, distributed above 100°C. These networks were installed with the purpose of reducing fuel consumption, as well as to integrate the energy generation through CHPs (Combined Heat and Power). The third generation was introduced in the 1980s and it's main difference was the use of a lower distribution temperature (below 100 °C). In those years

the main reasons for the installation of DH was security of supply, since they allowed to replace oil with more local and cheaper fuels such as coal, biomass and waste. Moreover, it allowed to use industrial waste heat, as an energy source.

Nevertheless, a distribution temperature between 70-100 °C still origins very high heat losses, and it does not allow to integrate a larger number of heat sources. Moreover, also in space heating systems in buildings, there has been an evolution towards lower operating temperatures, reducing the average demand temperature. These were the drivers for the development of the 4th generation, for which networks operate at a temperature between 30-70 °C. This enables a much better integration of the heating system into the global energy system, as it makes it possible to include low temperature sources (geothermal, solar thermal, refrigeration systems or waste heat from data centers).

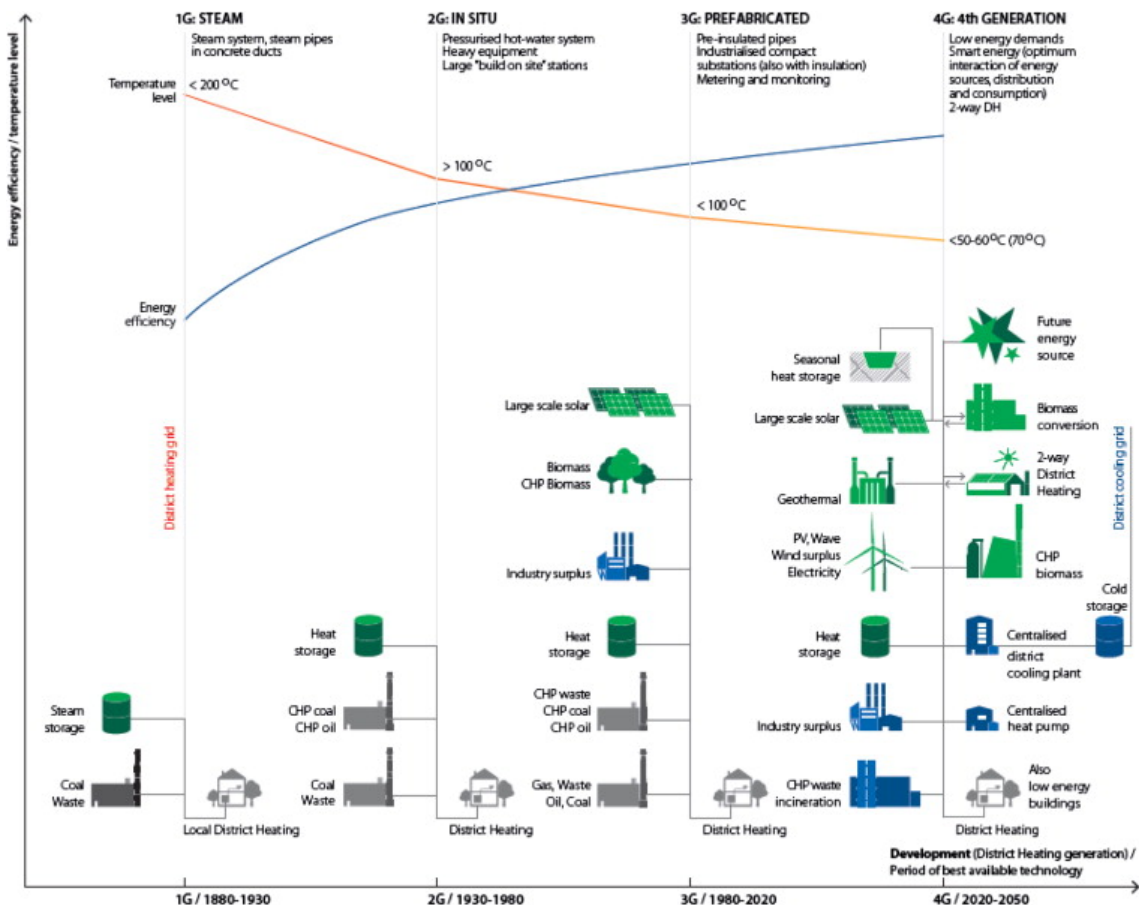


Figure 3: The evolution of the district heating technology, from the 1st to the 4th generation. Source: [?]

District cooling (DC) networks had a similar development as DH networks, although to a smaller extent.

## 2.2 Fifth generation district energy networks

The 4th generation of DH technology, has already achieved remarkable success and has been widely applied, especially in Europe. However, the exergy losses of the system are still very high, due to the diversity of heat levels present in the system, limiting its efficiency. Moreover, the integration of DC, which, as it was mentioned beforehand is already important in cities and will become more and more important throughout the next years, needs the installation of a second and separate networks, which leads to high upfront costs.

This has lead to the birth of a new technology that uses an even lower distribution temperature

(10-25 °C) to provide heating and cooling. In fact, the transfer fluid acts as cold network for cooling purposes and supplies, at the same time, evaporator heat to decentralized heat pumps. This is what is known as the 5th generation DH networks, also known as District Energy Networks (DEN) or District Heating and Cooling (DHC). Besides the higher energy and exergy efficiency, which reduce the operating costs, this technology also reduces the upfront costs. Given the lower distribution temperature, in fact, the pipes require less insulation, as well as they can be placed in shallower depth in the ground.

This technology has appeared in Switzerland in 2007, and it's mostly known as *anergy network*, or in german *Anergienetz*. To the authors knowledge, there are seven such systems operating by the end of the year 2018[?]. A summary of a selection of four of them is shown in Table 1, while more detailed information can be found in the Appendix 8.

Table 1: District energy systems in Switzerland

	<b>Anergienetz ETH Hönggerberg</b>	<b>Suurstoffi- Areal</b>	<b>Anergienetz Friesenberg (FGZ)</b>	<b>Genève-Lac- Nations (GLN)</b>
<b>Location</b>	Zürich	Rotkreuz	Zürich	Genève
<b>Year of construction</b>	2012 - 2026	2010 - 2020	2011-2050	2008 - 2016
<b>ERA [m<sup>2</sup>]</b>	475'000	172'421	185'000	840'000
<b>Inst. Heating capacity [kW]</b>	8'000	6'732	3'930	4'300
<b>Heating demand [MWh/a]</b>	28'450	10'619	35'000	5'000
<b>Inst. Cooling capacity [kW]</b>	6'000	2'327	3'500	16'200
<b>Cooling demand [MWh/a]</b>	26'200	2'364	80'000	20'000
<b>Distribution fluid</b>	water	water	water	water
<b>Heat source</b>	Laboratories waste heat +HP	Waste heat buildings + PVT (solar th.) +HP	Waste heat data center+HP	Lake water +HP
<b>Heat storage</b>	Geothermal well field (431 at 200m)	Geothermal well field (215 at 150 m, 180 at 280m)	Geothermal well field (332 at 250m)	None
<b>T of heating pipe</b>	24 °C - 8 °C	25 °C - 8 °C	28 °C - 8 °C	17 °C - 5 °C
<b>T of cooling pipe</b>	4 °C - 20 °C	4 °C - 17 °C	4 °C -24 °C	5 °C - 12 °C
<b>Tot. investments [Mio.CHF]</b>	37	n/a	42.5	33
<b>Tot. COP of heating (incl. Pumps...)</b>	5.8	2.7	4.1	6.5

All the anergy networks presented in Table 1 still base on water as a working fluid. Therefore, they work on sensible heat, which means that a heat exchange is bound to a variation in the fluids temperature. The challenge of these systems is given by the flow rate that is necessary to limit the temperature difference between the inlet and the return temperature of the network. Thus,

it could be very interesting to use refrigerants, instead of water, that enable to work with latent heat instead, which means collecting and distributing heat through the condensation, or the evaporation, of the refrigerant. This poses some additional technological challenges, but has also very clear advantages, as it will be shown in the next chapters.

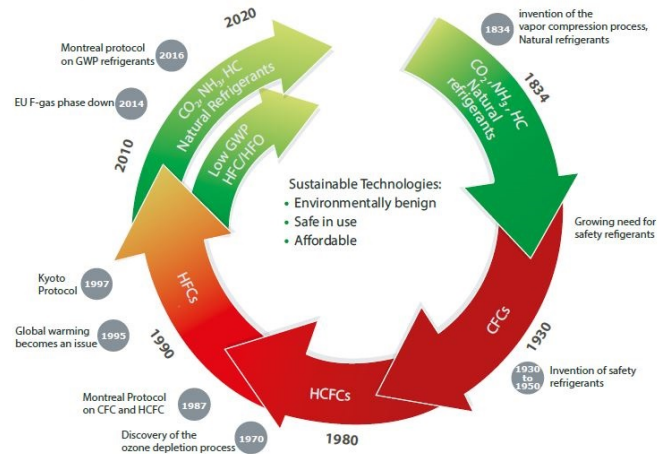


Figure 4: The historical cycle of refrigerants Source: [?]

The choice of the refrigerant strongly depends on the application. In function of the operating conditions, three main criteria are evaluated: affordability, safety and environmental impact. A summary of the history of refrigerants is shown in Figure 4. The Montreal protocol, signed in 1987, designed the phase out of HCFC and CFCs, in order to prevent ozone layer depletion. This boosted the use of HFCs, as a replacement. However, not far later, people realized that despite being less damaging to the ozone layer, they were powerful greenhouse gases. Since 2013, a federal ordinance also strongly restricts the use of these last ones in Switzerland[?]. Also Europe has planned the phase-out of HFC in 2014[?]. This means that today the choice of refrigerants is essentially limited to natural refrigerants - as for example CO<sub>2</sub> (R744), ammonia (R717) or propane (R290) - and the new environmentally friendly HFOs - as for example the fluorinated propane isomer R1234yf.

The choice of CO<sub>2</sub> as a refrigerant relies, besides its thermodynamic properties, on the following arguments[?]:

- it is very abundant in the environment and is also waste of a multitude of industrial processes
- it is harmless to the biosphere
- it is non-flammable and non-toxic
- it is an inert gas

In fact, according to Danfoss[?], CO<sub>2</sub> will dominate industrial refrigeration, together with ammonia. Already today, this technology is widely used. For instance Migros, Switzerland's largest retail company, opened its first supermarket to use CO<sub>2</sub>, in a low-temperature subcritical system, in 2002. By today, 411 of the 700 supermarkets in Migros's portfolio are equipped with transcritical CO<sub>2</sub> systems[?].

## 2.3 CO<sub>2</sub> DEN

### 2.3.1 The technology

Weber and Favrat [?] compared the performance of a DEN using subcritical CO<sub>2</sub>, the HFO R1234yf and water. They were able to show that the CO<sub>2</sub> network performs best, and has the biggest

potential for DEN systems[?]. As explained above, a refrigerant based DEN technology allows to store and transfer heat through the latent heat of vaporization of the refrigerant. The operating pressure is chosen in order to obtain the desired temperature in the system. That temperature is selected to be as high as possible to represent a good heat source for the decentralized heating heat pumps - resulting in good COP values -, while still allowing free cooling - avoiding the installation of compression chillers, and thus drastically reduce electricity consumption for space cooling.

The network consists of one saturated liquid pipe and of one saturated vapor pipe, both in a saturated temperature range from 12 to 18 °C[?]. The working principle is shown in Figure 5. Heating users can extract heat from the network through condensation of the refrigerant, taken from the vapour pipe. Respectively, cooling users take refrigerant from the liquid pipe and evacuate heat by evaporating it. The heat exchanges between the network and the users occur through condenser-evaporators heat exchangers, which keep the different refrigerant loops isolated[?]. The synergy between simultaneous heating and cooling users allows the recovery of waste heat. Most of the time, the required heating and cooling capacity will not be equal, which means that there is the need for a centralized balancing power. Indeed, a central plant is responsible to balance the overall network, by exchanging heat with the environment. For instance, a sole/water or a water/water heat pump can be used for this purpose.

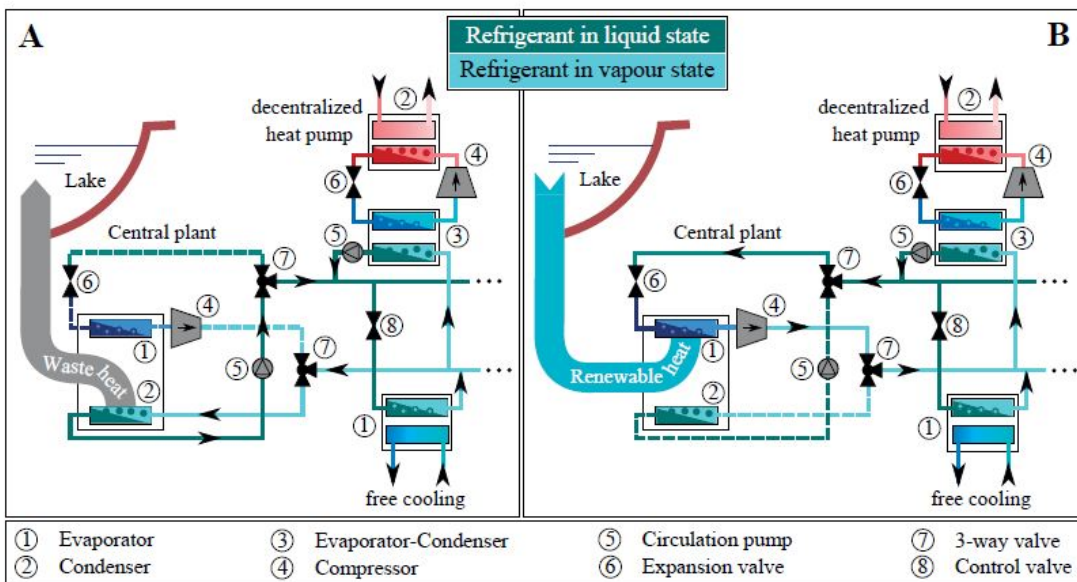


Figure 5: Schematics of a refrigerant based district energy network. Part A represents its net cooling operation, and part B its net heating operation. Source: [?]

One of the big advantages of this technology, with respect to water based DEN, is the pipes sizing. In fact, given the fact that it works on pressure maintenance instead of a fluid flow, no return pipe is necessary, which results in a slightly shorter total length of installed pipes. Moreover, due to the higher energy density of latent heat, the pipes diameter is drastically reduced. Henchoz et al. [?] compared three different working fluid on the same study case, showing that, while CO<sub>2</sub> needs pipes of only 280/330mm (liquid/vapor), R123yf would need 270/700mm and water 625/625mm. Given the low operating temperatures, there are much lower requirements for pipes insulation. While water pipes need to be buried deep enough to prevent damage due to water freezing, in case part of the network had to be stopped during winter, CO<sub>2</sub> does not freeze and thus does not require a minimum freeze-safe depth. Henchoz et al. have even imagined installing the pipes inside a sidewalk module, which would drastically simplify maintenance and inspection. Given the smaller diameter, it would also be possible to retrofit an old, high temperature district heating network, by placing the CO<sub>2</sub> pipes inside the old water pipes. All the above mentioned advantages of using CO<sub>2</sub>, result in lower upfront costs.

CO2den:  
necessary to talk about the advantage of expanding network with additional compressor easier than for water??

CO2den:  
need more drawbacks?  
or write more about it?

CO2gva:  
Talk about financial numbers comparison?  
Otherwise delete fig 8

The main drawback of this technology is the high operating pressure, which situates at about 50 bars, and the safety concerns that could derive from the large amount of CO<sub>2</sub> that could escape in case of a major leakage. Nevertheless, as described in 2.2, CO<sub>2</sub> refrigeration networks are already widely used in supermarkets, and the technology is considered as safe.

### 2.3.2 Performance

Henchoz et al.[?] performed an analysis of the potential application of a CO<sub>2</sub> based DEN in a district in the city of Geneva. A map of the district, called "Rues basses", is shown in Figure 6.

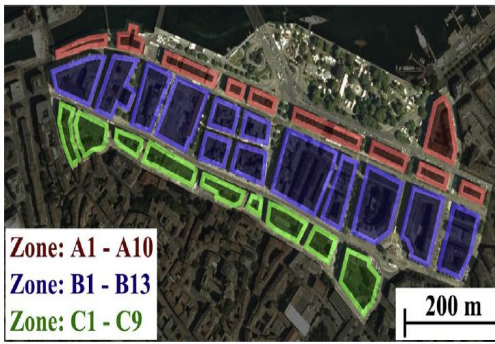


Figure 6: Representation of the the studied area and of its subdivision into 32 zones.  
Source: [?]

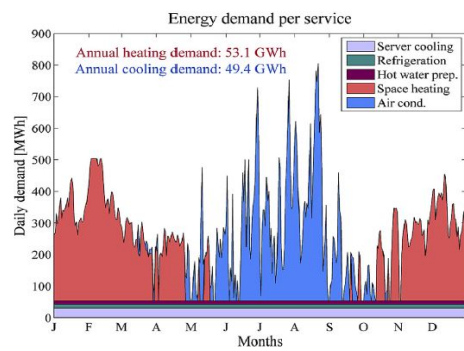


Figure 7: Energy demand for the area studied over the year 2012. Source: [?]

Table 2 shows the distribution of building affectations - which is important to determine the energy consumption - in the studied area. The total ERA is 687'800m<sup>2</sup>.

Table 2: Distribution of the energy reference area for the different zones and building affectations

Zones	Commercial [m <sup>2</sup> ERA]	Offices [m <sup>2</sup> ERA]	Residential [m <sup>2</sup> ERA]
A1 - A10	20'700	89'200	17'700
B1 - B13	97'000	260'700	61'600
C1 - C9	40'400	62'600	48'100
Relative share	23%	60%	17%

The energy demand of heating (53.1GWh/yr) and cooling (49.4GWh/yr) in the studied area is shown in Figure 7. Throughout the year, the district presents nearly the same heating demand as for cooling, but they happen in different seasons.

The proposed CO<sub>2</sub> based DEN is balanced by a central plant - a heat pump - that exchanges heat with the nearby lake. In order to benchmark the results, this technology has been compared to a traditional heating and cooling system, based on oil boilers and cooled compression chillers.

The results are remarkable. In fact, the CO<sub>2</sub> based DEN shows a final energy consumption of 10,968 MWh of electricity, which corresponds to a reduction of 84.4 %, with respect to the reference scenario. Its exergy efficiency situates between 40-45%.

### 2.3.3 Integration in smart energy system

The integration of high shares of renewable energies represents an important challenge. In fact, it requires a lot of slack to handle the volatile nature of renewable energy sources like wind or sun. On one side, this slack will be mainly given through a smart control of the electricity grid

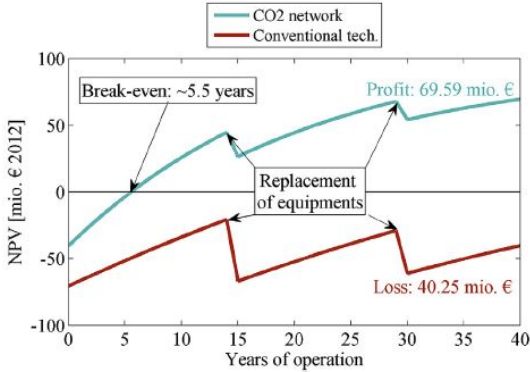


Figure 8: Evolution of the net present value over the lifetime of the two energy conversion technologies. Source: [?]

on multiple levels. It starts from the demand side management (DSM) inside households, through optimization at district level, up to a national and international control. These decentralized grids, or grid controls, are called *smart grids*.

With the vast success of heat pumps throughout the last decade, the control of electricity grids is more and more interconnected with the production of heat. This further complexifies the system by adding a level of constraints, but it also opens new levels of control. Indeed, if well designed, a DEN offers an additional level of slack that can be used in combination with the smart grid, multiplying control power. The CO<sub>2</sub> DEN offers several possibilities to shift the loads, relieving the grid.

On one hand, it simplifies the deployment of a smart control of the heat pumps, which can strongly contribute in the DSM. The decentralized heat pumps can make use of a buildings thermal inertia to adapt electricity use to energy availability. CO<sub>2</sub> vapor and liquid storage can act as a buffer, enabling load-shifting also for the central plant of the DEN. Sizing of these storage capacities will determine the possible time-span that the shift can achieve. Given the low distribution temperature, this approach also facilitates the storing of heat, as for example in a geothermal field.

On the other hand, the use of CO<sub>2</sub> as a refrigerant for the network could improve the integration of a power to gas (PtG) system. Indeed, one big challenge in the future, especially in higher latitudes, where seasonal variation are consistent, is to ensure energy supply during winter season, when, due to shorter and weaker solar irradiation, PV panels produce less. It is thus important to find a way to store the excess of renewable energy production during the summer, in order to use it in the winter. One solution to do that is PtG, which defines the process of transforming electrical power to a gas, like methane, which is easy to store. To do so, electricity is used to produce hydrogen, which can be combined with CO<sub>2</sub> to form Methane, in a process called methanization. Methane can be used during the winter to produce electricity and heat, in a combined heat and power plant (CHP), as for example a SOFC, a gas turbine, or a combination of them. For this reason, PtG is widely studied across Europe and many such plants have already been built.

Suci et al. [?] studied the synergy between a CO<sub>2</sub> based DEN, decentralized PV and such a PtG system. The CO<sub>2</sub> network could be used to store the carbon dioxide, which is captured from CHPs or industrial processes during winter, needed for methanization. At the same time, the DEN can directly use and dispatch the heat produced from the CHPs. In their work, they analyzed the PV area, and thus the investment, required to achieve a completely autonomous energy system, for different European climatic zones. The results showed that decarbonized autonomous energy systems based on DENs and PtG tecnologies are possible, along with a very broad deployment of solar energy. It is also shown that the payback time of such a system is between 11 and 14 years, which makes it very attractive also from an economic point of view.

## 2.4 Direct-expansion ground source heat pump

where to put  
this section?

For heat pumps based systems, sourcing heat from the sole, instead of from the ambient air, is a very interesting solution at our latitudes, especially, as it has been seen, for integration of a 5th generation DEN, since it improves heating and cooling COPs, and, to a certain extent, it allows heat storage. In traditional Ground-Source Heat Pumps (GSHP), the heat pump and the ground are connected by means of a closed loop, using water, or a water solution. This system, called the secondary loop GSHP (SL-GSHP), is shown on the right side of Figure 9. However, it has been proved [?, ?] that the system efficiency can be improved, by allowing to directly expand the refrigerant into the ground and thus let the ground act as a condenser/evaporator. Shown on the left side of Figure 9, this system is called Direct Expansion GSHP (DX-GSHP).

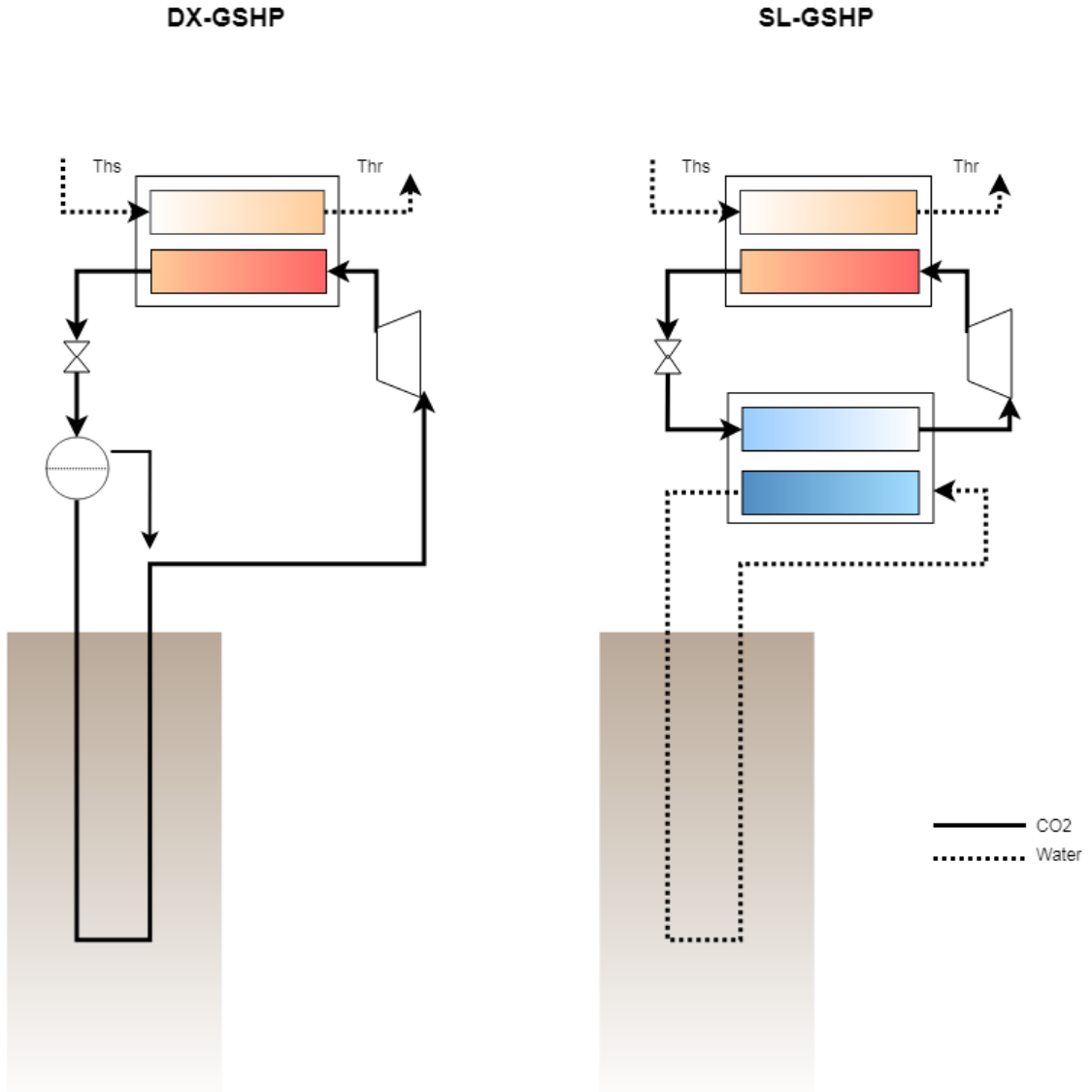


Figure 9: A simplified schematics of the two GSHP technologies

So far, this technology is not so widely spread, mostly because of a more demanding system design and, because of the risk of environmental pollution, when non-natural refrigerants are used. Indeed, literature about DX-GSHP is still scarce, especially for CO<sub>2</sub> as a refrigerant. There are only few numerical CO<sub>2</sub>-DX-GSHP studies [?, ?, ?, ?], which are not yet sufficient to obtain a scientific appreciation of the technology. Nevertheless several prototypes and experimental set-ups have been built and analyzed [?, ?, ?], proving a higher efficiency of the DX, with respect to a SL.

One of the main reasons for this efficiency gain is the elimination of the temperature lift of the

water loop, which is replaced by a constant temperature phase-change, as well as the elimination of the minimum approach temperature necessary to exchange heat between the SL and the heat pump. This results in a higher COP for the heat pumps. Moreover, CO<sub>2</sub> presents a higher heat transfer coefficient, which again allows to either reduce the minimum approach temperature, or extract a higher power with respect to an equal exchange surface. The minimum approach temperature has to be determined in function of the thermal permeability of soil and is correlated to the length and total surface of the geothermal probes, as well as the refrigerant flow rate.



## 2.5 optimization

### 2.5.1 MILP

Mixed integer linear programming (MILP) is...  
AMPL a programm, solver using Gurobi, GLPK...  
Black box??.....

State variables  $X_{state}$   
Model  $F_{X_{state}}$   
Context specification  $S_{X_{state}}$   
Inequality constraints  $G_{X_{state}}$

find cheat-sheet of exam MOES to do that

## 2.6 Osmose

IPESE developed in-house software for this Lua language Layers, ETs... Equations (mass balances, resource balances, heat cascade...) Creates mod files for ampl optimization Postcompute to export Energy conversion technology sizing.

$$f_{u,t} \leq f_u \quad \forall u \in U, \forall t \in T \quad (1)$$

$$f_u^{min} \cdot y_u \leq f_u \leq f_u^{max} \cdot y_u \quad \forall u \in U \quad (2)$$

(3)

For *process units*, only the houses,  $y_u = f_u^{min} = f_u^{max} = 1$

Heat cascade A set of equations, called heat cascade, makes sure that heat is always transferred from a higher temperature to a lower one, also considering the respective minimum approach temperature for each stream.

$$\sum_u^U f_{u,t} \cdot \dot{Q}_{u,t,k} + \dot{R}_{t,k+1} - \dot{R}_{t,k} = 0 \quad \forall k \in K, \forall t \in T \quad (4)$$

$$\dot{R}_{t,k} \geq 0 \quad \forall k \in K, \forall t \in T \quad (5)$$

$$\dot{R}_{t,1} = \dot{R}_{t,k+1} = 0 \quad \forall t \in T \quad (6)$$

(7)

is third eq  
rtk+1 = 0  
correct???

Mass balances The demand  $\dot{m}_{r,u,t}^+$  and the supply  $\dot{m}_{r,u,t}^-$  of resource  $r \in R$  of each unit  $u \in U$  is computed.

$$\dot{M}_{r,u,t}^- = \dot{m}_{r,u,t}^- \cdot f_{u,t} \quad \forall r \in R, \forall u \in U, \forall t \in T \quad (8)$$

$$\dot{M}_{r,u,t}^+ = \dot{m}_{r,u,t}^+ \cdot f_{u,t} \quad \forall r \in R, \forall u \in U, \forall t \in T \quad (9)$$

(10)

The balance of each resource has to be respected.

$$\sum_u^U \dot{M}_{r,u,t}^- = \dot{M}_{r,u,t}^+ \quad \forall r \in R, \forall t \in T \quad (11)$$

Electricity is also balanced

$$\dot{E}l_{houses}^+ + \dot{E}l_{heating}^+ + \dot{E}l_{cooling}^+ + \dot{E}l_{grid}^+ = \dot{E}l_{PV}^- + \dot{E}l_{grid}^- \quad (12)$$

Optimization function

$$\min (TotalCost) = \min (CAPEX + OPEX) \quad (13)$$

$$\min \sum_u^U \dots \quad (14)$$

(15)

$$\min (Operatingcost) \quad (16)$$

$$\min \sum_u^U \left[ \sum_{t=1}^T \left( c_u^{op1} \cdot y_{u,t} + c_u^{op2} \cdot f_{u,t} + C_{el}^- \cdot \dot{E}l_{grid,t}^- - C_{el}^+ \cdot \dot{E}l_{grid,t}^+ \right) \cdot t_t^{op} \right] \quad (17)$$

(18)

where  $c_u^{op1}$  and  $c_u^{op2}$  are the respectively the fixed and the variable operating cost, and  $C_{el}^-$  and  $C_{el}^+$  are the buying and selling price of electricity.

ET energy technologies:

The needed parameters are:

- cinv1: fixed part of the IC, given in [CHF/year]. This can be found in figure 10;
- cinv2: variable part of the IC, given in [CHF/year]. This can be found in figure 10;
- cop1: fixed part of the OC, which corresponds to maintenance and service costs.
- cop2: variable part of the OC. This is calculated by the solver, also in [CHF/h].

### 3 Methodology

#### 3.1 Energy demand / Typical days

According to SIA standards

Threshold temperature for heating or cooling

The optimization of an energy system is commonly performed over the time span of one year, in order to account for the different seasons. However, this requires a very long computing time, given the high number of timesteps. Thus, it is used to group similar days, according to a set of parameters as for example temperature or irradiation, into so called typical days. The days can be clustered in different ways. It can be chosen to compute an average day for each month or some

add this paragraph

machine learning clustering algorithm - as for example K-means, DBSCAN or GMM - can be used to group the days into the desired number of clusters. The resulting typical days correspond to a period  $p$ , with a number of times  $t$ , as explained in section 2.6. In order to account for the data compression, a value called *occurrence* indicates how many times a given typical day occurs, i.e. how many times a given period occurs.

Two additional days with the two opposite extreme temperature conditions are added to the typical days, in order for the model to account for them in the equipment sizing. To avoid a bias of the operation results, those days are set with an occurrence of zero.

### 3.2 Geothermal wells

The most important parameter in geothermal wells is the soil temperature, which is normally constant throughout the year. In fact, only the first 10 meters are influenced by the temperature of the air[?]. Moreover, the temperature increases with depth. According to the SIA norm SIA384[?], the mean temperature in a geothermal well can be calculated by:

$$T_{g,mean} = T_{g,sup} + \frac{L_w \cdot \nabla T_g}{2} \quad (19)$$

where  $T_{g,sup}$  is the ground temperature at the surface,  $L_w$  is the length of the well and  $\nabla T_g$  is the temperature gradient of the soil.

As for other technologies, the energy demand of the circulating pumps is assumed to be negligible.

### 3.3 Investment cost function

To calculate the investment cost for a given technology, it is possible to interpolate data from available products on the market. However, it is also possible to evaluate a cost function, according to a standard procedure in industrial processes[?].

First, it is necessary to calculate the cost of purchase of the unit, in function of its size, given by the sizing power, which can be the electrical power  $E$ , the delivered heat  $Q$  or the area of a heat exchanger  $A$ .

$$C_{pex} = \frac{I_t}{I_{t,ref}} \cdot 10^{(k_{1,ex} + k_{2,ex} \cdot \log(E/Q/A))} \quad (20)$$

Through a factor called *Bare Module Factor*, the accessory costs of transport, installation, connection are included in the calculation, obtaining the total investment costs

$$CBM_{ex} = C_{pex} \cdot FBM_{ex} \cdot e \quad (21)$$

where  $e$  is the currency ration from USD to CHF. The annuities are calculated with the annuitization factor ( $af$ ) by the following formula, where  $n$  is the assumed lifetime of the equipment in years, and  $i$  the interest rate.

$$IC_{yearly,ex} = CBM_{ex} \cdot af \quad af = \frac{i \cdot (1+i)^n}{(1+i)^n - 1} \quad (22)$$

This investment cost function is not a linear function. However, as described in Section 2.6, to solve the MILP it is necessary to provide a set of linear parameters that approximate the function. These are found by linearizing the investment cost function around the reference value, defined in the range of application. This was done with help of a matlab code, using *polyfit* and *polyval* functions. Figure 10 shows the linearized function with the according cost parameters.

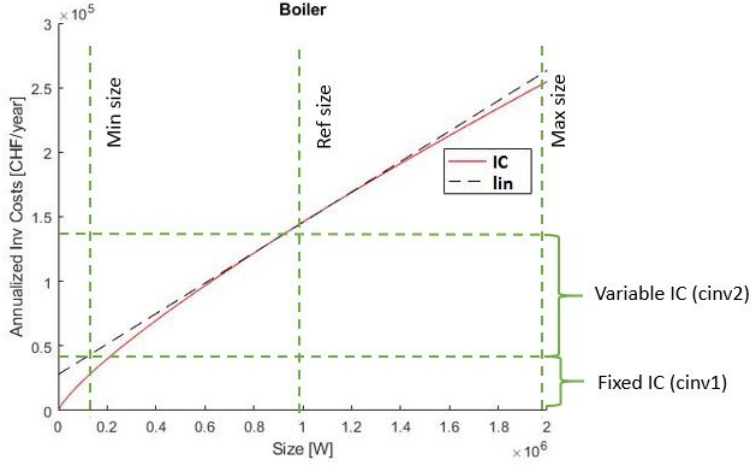


Figure 10: Linearization of investment cost function

### 3.4 Minimum approach temperature

The critical sizing parameter for a heat exchanger is the minimum approach temperature  $\Delta T_{min}$ , which corresponds to the smallest temperature difference in the heat exchanger between the hot and the cold stream, as shown in Figure 11. This value is strongly dependent from the heat exchanger area  $A_{ex}$  and the heat transfer coefficients  $h$  of the exchanging fluids. They are correlated in the following way:

$$A_{ex} = \frac{Q_{ex}}{U \cdot LMTD} \quad (23)$$

$$LMTD = \frac{(T_{Hot,in} - T_{cold,out}) - (T_{Hot,out} - T_{cold,in})}{\log \left( \frac{T_{Hot,in} - T_{cold,out}}{T_{Hot,out} - T_{cold,in}} \right)} \quad (24)$$

$$T_{Hot,in} = T_{cold,out} + \Delta T_{min} \quad (25)$$

where  $LMTD$  is the logarithmic mean temperature difference and  $T$  are the inlet and outlet temperatures of the hot and cold streams, as shown in Figure 11. The overall heat transfer coefficient is given by [?]:

$$U = \frac{1}{\frac{1}{h_{(hot)}} + \frac{\Delta x_{wall}}{k_{wall}} + \frac{1}{h_{(cold)}}} \quad (26)$$

where  $h_{(hot)}$  and  $h_{(cold)}$  are the heat transfer coefficient of the hot and cold fluid, while  $\Delta x_{wall}$  and  $k_{wall}$  are respectively the thickness and the thermal conductivity of the heat exchanger plates.

A bigger  $A_{ex}$  allows a smaller  $\Delta T_{min}$ , which increases the investment costs but lowers the operating costs, and the other way around. Therefore, an optimum can be found for each specific application. The optimization is done by minimizing the total cost, which include the operating costs of a heat pump - whose COP decreases with  $\Delta T_{min}$  -, and the investment costs of the heat exchanger and of the HP:

$$\min_{\Delta T_{min}} \{OC(\Delta T_{min}) + IC(\Delta T_{min})\} \quad (27)$$

Heat transfer coefficients used are shown in Table 3. The values for R134yf [?] while for CO<sub>2</sub> from this paper[?]. Validated also by comparison between the two[?].

dtmin finish  
rewriting  
this last part

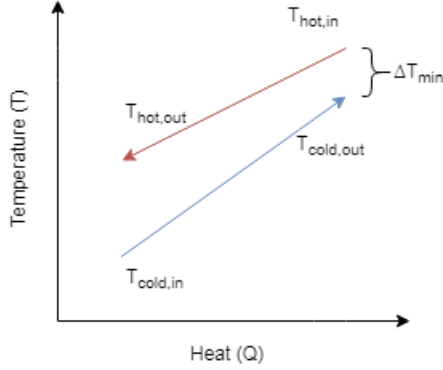


Figure 11: Minimum approach temperature in a counter-flow heat exchanger.

Table 3: Heat transfer coefficients found in literature

Fluid	Water	R134yf	R744
$h[W/(mK)]$	600	3000	7000

### 3.5 Exergy

The exergy of an energy transfer is defined as the maximum amount of work that can be extracted from it, through reversible transformations that exchange with the environment. Thus the calculation of exergy losses is a very interesting indicator to analyze a given process or system, since it expresses the quality and the efficiency with which the system operates, with respect to the maximum possible. Therefore, other as for the coefficient of performance, these values are always lower than 100 %.

The exergy value, i.e. the maximum work that can be extracted from an energy transfer, is derived from the first two thermodynamic principles, and is given by the following formula:

$$\dot{E}_{max}^- = \sum_i \dot{Q}_i^+ \left(1 - \frac{T_a}{T_i}\right) + \sum_r \dot{M}_r^+ (h_r - T_a s_r) \quad (28)$$

The exergy losses are thus given by the difference between the exergy value and the energy furnished to the system:

$$\dot{L} = \dot{E}_{max}^- - \sum_j \dot{E}_j^- \geq 0 \quad (29)$$

$$\dot{L} = (1 - \eta_{exergy}) \dot{E}_{max}^- \quad (30)$$

In our case this can be written as:

$$\eta_{exergy} = \frac{\dot{E}_{grid}^- + \dot{E}_{hot,r}^- + \dot{E}_{cold,a}^-}{\dot{Q}_{grid}^+ + \dot{Q}_{hot,a}^+ + \dot{E}_{grid}^+} \quad (31)$$

$$\dot{L} = (1 - \eta_{exergy})(\dot{E}_{grid}^+ + \dot{E}_{hot,a}^+ + \dot{E}_{cold,r}^+) \quad (32)$$

where  $\dot{E}q$  are the exergy value of hot and cold streams, respectively above (a) and below (r) the ambient temperature.  $E_{grid}^+$  and  $E_{grid}^-$  are the electricity bought from and sold to the grid.

### 3.6 Energy technology models

The models for the energy technologies are adapted from the source code written by Suciu Raluca. thermodyn cycle from[?]

cite anything, or name is enough?

other names?

### 3.6.1 Heat pumps - basic (Carnot)

Heat pumps can be modeled in a simple way, using the principle of the Carnot cycle, with help of the following equations:

$$\dot{E}_{compressor} = \frac{\dot{Q}_{cond}}{COP_{real}} = \frac{\dot{Q}_{evap}}{\eta_{COP} \cdot COP_{theoretical}} \quad (33)$$

$$COP_{theoretical,heating} = \frac{T_h}{T_h - T_c} \quad COP_{theoretical,cooling} = \frac{T_c}{T_h - T_c} \quad (34)$$

where  $\dot{Q}_{cond}$  is the heat delivered and  $\dot{Q}_{evap}$  the heat sourced by the heat pump.  $\eta_{COP}$  is an experimentally defined efficiency to account for irreversibility of the cycle, i.e. to give the ratio between the theoretical and the real COP. The values used in this work are shown in Table 4, calculated by Girardin et al.[?], based on values obtained from c heat pump certification center[?].

Table 4: Theoretical efficiency factor for COP

Type	Size	$\eta_{COP}$
Air/Water	Decentralized	0.34
CO <sub>2</sub> /Water	Decentralized	0.43
Ground/Water	Decentralized	0.43
Ground/Water	Centralized	0.55
Water/Water	Centralized	0.55

### 3.6.2 Heat pumps - detailed (Thermodyn.)

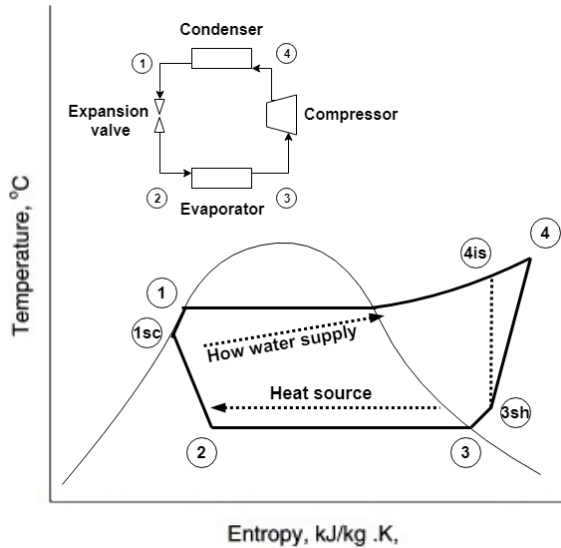


Figure 12: Temperature–entropy diagram of a R134yf based heat pump system.

Given the comparison between new and efficient technologies, the differences of performance are relatively small and it might be necessary to provide a more accurate model of the heat pumps, that are able to correctly represent and calculate the operating cycles and conditions. This can be done by modeling the thermodynamic cycle, represented in Figure 12:

**1 - 2** : Expansion to low pressure level

**2 - 3** : Evaporation by cooling down the heat source

**3 - 3sh** : Superheating in evaporator

**3sh - 4** : Compression to high pressure level

**4 - 1** : Condensation of refrigerant, delivering heat

The compressor is a crucial component for the design of a heat pump, since it has the largest share of impact on the energy efficiency. To calculate its efficiency, the model of Hu et al.[?] has been used. The shaft power can be computed in function of the isentropic efficiency ( $\eta_{is}$ ) by:

$$W_{shaft} = \frac{\dot{m}(h_{d,is} - h_s)}{\eta_{is}} \quad (35)$$

where  $h_{d,is}$  is the isentropic discharge enthalpy and  $h_d$  is the suction enthalpy. The compressors input power is expressed in function of its mechanical efficiency ( $\eta_{mech}$ ) by:

$$E_{comp} = \frac{W_{shaft}}{\eta_{mech}} \quad (36)$$

The efficiency of the compressor is thus calculated as:

$$\eta_{comp} = \frac{\text{isentropic work of compression}}{\text{actual work of compression}} = \frac{\dot{m}(h_{d,is} - h_s)}{E_{comp}} = \eta_{is}\eta_{mech} \quad (37)$$

The numerical values of those efficiencies are strongly dependent from the ratio between the pressure of discharge  $P_d$  and the pressure of suction  $P_s$  of the compressor. They can be computed inside the model with help of the relations obtained by Li et al.[?]:

$$\eta_{mech} = 0.85 \quad (38)$$

$$\eta_{is} = 0.874 - 0.0134 \cdot \left(\frac{P_d}{P_s}\right) \quad (39)$$

$$(40)$$

The expansion of the refrigerant in the expansion valve is assumed to be isenthalpic.

Thus, the procedure to evaluate the operating conditions of the heat pump is the following:

1. calculate thermodynamic state in point (1) knowing the evaporation temperature  $T_{evap}$  and assuming saturated liquid
2. calculate thermodynamic state in (1sc) using same pressure as in (1), with  $T = T_{evap} - \Delta T_{subcool}$
3. calculate thermodynamic state in point (3) knowing the evaporation temperature  $T_{cond}$  and assuming saturated vapor
4. calculate thermodynamic state in (3sh) using same pressure as in (3), with  $T = T_{cond} + \Delta T_{superheat}$
5. calculate thermodynamic state in (2), assuming isenthalpic expansion of the valve, with  $H_2 = H_{1sc}$  and  $P_3$
6. calculate isentropic efficiency of compressor  $\eta_{c,is}$ , knowing the discharge pressure  $P_1$  and the suction pressure  $P_3$
7. calculate thermodynamic state in (4is), assuming an isentropic compression with  $S_{3sh}$  and  $P_1$
8. calculate thermodynamic state in (4), accounting for the isentropic efficiency of the compressor  $\eta_{c,is}$ , using  $H_4 = H_{3sh} + \frac{H_{4is} - H_{3sh}}{\eta_{c,is}}$ , and  $P_{1sc}$ .

In Osmose, these values are calculated with help of *Coolprop*, which is an open-source database of fluid and humid air properties that allows to calculate operating conditions for a large number of fluids and refrigerants. Thanks to a *lua wrapper*, which is a *lua* module that provides an API to the external software, *Coolprop* is called inside Osmose.

The electrical power of the heat pump and its COP, are then calculated by:

$$E_{el} = \frac{m_{ref} \cdot (H_4 - H_{3sh})}{\eta_{mech}} \quad (41)$$

$$Q_{cond} = m_{ref} \cdot (H_4 - H_{1sc}) \quad (42)$$

$$COP = \frac{Q_{cond}}{E_{el}} \quad (43)$$

where  $m_{ref}$  is the massflow of refrigerant in the heat pump.

### 3.6.3 Heat pump - supercritical CO<sub>2</sub>

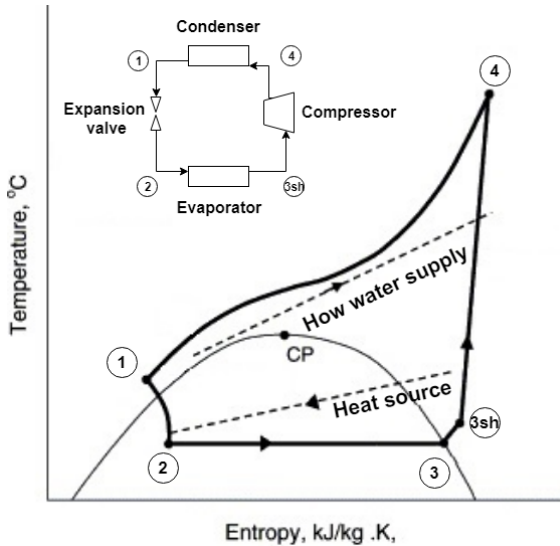


Figure 13: Temperature–entropy diagram of a trans-critical CO<sub>2</sub> heat pump system for a domestic hot water production. Source: [?]

In traditional heat pumps, the heat delivery occurs through condensation of the refrigerant, which happens at a fixed temperature. This originates high exergy losses, especially in processes where a high temperature lift is needed in the gas cooler. Some refrigerants have the particular property of having a very low critical point. Among others, a very interesting one is CO<sub>2</sub> - technically known as R744 -, which has a critical point at 74 bars and 31 °C[?]. As explained in Section 2.2, CO<sub>2</sub> is also a very interesting choice for environmental and financial reasons.

The supercritical cycle is shown in Figure 13, represented on the temperature-entropy diagram. The different steps of the process are explained hereafter:

**1 - 2** : Expansion to low pressure level

**2 - 3** : Evaporation by cooling down the heat source

**3 - 3sh** : Superheating in evaporator

**3sh - 4** : Compression to transcritical pressure

**4 - 1** : Gas cooling in transcritical area, to heat water

Note that, as there is no phase change, the heat exchanger is called gas cooler, instead of condenser.

Even though the technological development is slowly closing the gap, CO<sub>2</sub> compressors have lower isentropic efficiency and lower volumetric efficiency than subcritical ones[?]. This comes from the high irreversibility caused by the superheated vapor horn and the high throttling losses[?]. However, transcritical operation also allows heat to be exchanged on a varying temperature, and the heat pump can be designed to fit the heat demand stream, optimizing exergy efficiency. This is particularly interesting in exchanges that require high temperature lifts, as in the case of domestic hot water heaters. In fact, this can be seen in Figure 13, between point 2 and 3. For instance, Stene et al. show that COP for a CO<sub>2</sub> HP is lower if it is used in subcritical range - for Space Heating (SH) (35/30 °C) - than in supercritical range - Domestic Hot Water (DHW) (10/60 °C) -, despite the much higher temperature difference. They also show that the resulting COP for DHW application outperforms conventional HPs[?].

For the transcritical CO<sub>2</sub> heat pump, the numerical values of the compressor efficiencies computed with help of the relations obtained by Wang et al [?]:

$$\eta_{mech} = 0.64107 + 0.07487 \cdot \left( \frac{P_d}{P_s} \right) \quad (44)$$

$$\eta_{is} = 0.8014 - 0.04842 \cdot \left( \frac{P_d}{P_s} \right) \quad (45)$$

$$(46)$$

The procedure to evaluate the operating conditions of the heat pump is the following:

1. calculate thermodynamic state in (1) with help of the temperature at the outlet of the condenser  $T = T_{cond,out} = 15.5^\circ\text{C}$ , optimized for this specific cycle by Henchoz et al.[?], and the pressure  $P_{cond,out} = 84.9\text{bar}$ , optimized to satisfy the required inlet temperature of the condenser
2. calculate thermodynamic state in point (3) knowing the evaporation temperature  $T_{evap}$  and assuming saturated liquid
3. calculate isentropic efficiency of compressor  $\eta_{c,is}$ , knowing the discharge pressure  $P_1$  and the suction pressure  $P_3$
4. calculate thermodynamic state in (4is), assuming an isentropic compression with  $S_{3sh}$  and  $P_1$
5. calculate thermodynamic state in (4), accounting for the isentropic efficiency of the compressor  $\eta_{c,is}$ , using  $H_4 = H_{3sh} + \frac{H_{4is} - H_{3sh}}{\eta_{c,is}}$ , and  $P_{cond,out}$ .
6. calculate thermodynamic state in (2), assuming isenthalpic expansion of the valve, with  $H_2 = H_1$  and  $P_3$

The equations to calculate electrical power of the heat pump and its COP, are the same as in Section 3.6.2.

### 3.6.4 Cooling tower / Air cooler

A cooling tower is an equipment used to cool down a stream through the ambient air. This is used for example in air conditioning systems, to evacuate the heat into the environment. It consists of a set of fans that blow the air through a heat exchanger. These fans originate a parasitic power consumption that can be calculated with help of the following equation[?]:

$$E_{fans}^{\cdot} = \frac{0.605 \cdot \dot{Q}_{cond}}{(\Delta T_{air} + \Delta T_{min}^{ref/air})^{0.9937}} \quad (47)$$

Where  $\dot{Q}_{cond}$  is the heat to be dissipated in the environment by the condenser.

### 3.6.5 Geo-cooling

Geo-cooling is the use of fresh temperatures of the ground for space cooling. This happens by simply circulating a fluid between the buildings, where the heat is extracted, and the geothermal wells, where heat is released into the ground. In practice, this happens by bypassing the heat pumps and making the water of the secondary loop (geothermal loop) directly exchange with the heating water loop. Investment costs are, thus, limited to an additional heat exchanger. As for the other units, the energy needed for circulation pumps is assumed to be negligible.

### 3.6.6 PV

The efficiency of the PV panels  $\eta_{PV}$  is given by the following equation:

$$\eta_{PV} = \eta_{ref} - \eta_{var}(T_{panel} - T_{ref}) \quad (48)$$

where  $\eta_{ref}$  and  $\eta_{var}$  are respectively the fixed efficiency and the temperature dependent efficiency. The temperature of the panel  $T_{panel}$  is calculated by means of:

$$T_{panel} = \frac{U_{glass} \cdot T_{amb} + GI \cdot f_{glass} - \eta_{ref} - \eta_{var} \cdot T_{ref}}{U_{glass} - \eta_{var} \cdot GI} \quad (49)$$

where  $U_{glass}$  is the thermal transmittance of the front glass,  $f_{glass}$  is the light transmittance of the front glass and GI is the global irradiation. Thus, the produced energy is given by:

$$E = GI \cdot A_{PV} \cdot \eta_{PV} \quad (50)$$

The area of installed PV  $A_{PV}$  is limited by the maximum available roof area multiplied by the area factor  $f_{area}$ , which for flat roofs is assumed to be  $\frac{1}{4}$ :

$$A_{PV} = A_{roof} \cdot f_{area} \quad (51)$$

### 3.6.7 Network

The length is calculated, according to a simplified method[?], with the following equations:

$$L = 2(n_b - 1)K \sqrt{\frac{S}{n_b}} \quad (52)$$

with  $S$  being the land area,  $n_b$  the number of buildings. The constant  $K$  is chosen at 0.5. And diameter of the pipes:

$$d = \sqrt{\frac{4 \cdot \dot{m}}{\pi v_s \rho}} \quad (53)$$

assuming a sizing velocity  $v_s$  of 3 m/s. The investment costs are calculated accordingly:

$$C = \sum_{k=1}^{n_b} \frac{L}{n_b} (c_1 d \sqrt{n_b + 1 - k} + c_2) \quad (54)$$

where  $c_1 = 5670$  and  $c_2 = 613$ .

Operating temperature is assumed to be 13/15 °C. Henchoz[?] has 10-12.5 for summer and 22.5 for winter!!!

The pressure losses, and thus the energy needed for the maintaining of the pressure, are assumed to be negligible.

how has this temperature been chosen? is there a paper? see henchoz with other T

## 4 Application

### 4.1 Case-study Eglantine

In the framework of the collaboration between Romande Energie and IPESE, a case study shall bring a concrete numerical case study into the discussion. For this, Romande Energie has chosen a real life example of a district in the city of Morges. This district is in the planning phase, and Romande Energie had worked on it, in order to participate in the call for tender. This case study shall be fertile ground to discuss the CO<sub>2</sub> DEN technology and its role in the future energy systems in Switzerland and, more particularly, in the future plans of Romande Energie.

#### 4.1.1 Context



Figure 14: Localization of the terrain, at the town scale. Source: [www.geo.vd.ch](http://www.geo.vd.ch)

The “Eglantine” is a terrain in the western part of the city of Morges, as shown in Figure 14. It is located in proximity of the key urban facilities, as well as it is close to the countryside. This terrain, which was partly used for agriculture, and partly covered by rich vegetation, belongs to the municipality, who is planning to use it for the urban expansion. At the municipality, they had the vision of building a new district, which would be planned to be exemplary in the sustainable development. After many years of revising and fine-tuning the land-use plan and its vision for the future, in the beginning of 2016, the commune launched a call for tender for the planning of the different aspects of the district. The call for tender regarding the energy system was opened by Losinger Marazzi the 1st December 2017, with a due date the 31 January 2018. The contract with the winner, unknown to the author, has been signed in the end of March 2018.

The call for tender requires the development of a complete energy system, including thermal and electrical energy. Estimated data about the buildings is provided, as seen in Table 5. Those are based on the following assumptions:

- All buildings are certificated Minergie 2017
- Space heating and hot water energy demand follow the SIA 380/1 and SIA 2031 norms
- Air ventilation is defined according to Minergie 2017 principles.
- Installed power values are calculated according to SIA 2024 norm

#### 4.1.2 Buildings

The district, which will host around 1'500 people, is composed of thirteen buildings, as shown in Figure 15, which account for a total energy reference area (ERA) of around  $47'000m^2$ . The details are shown in Table 5. According to the Minergie standard, the district will require about  $1.40MWh/yr$  for SH and  $0.95MWh/yr$  for DHW.

Table 5: Estimated energy demand in call for tender

Building	Energy Ref. Area (ERA)	Inhabitants	Space Heating (SH)	Hot Water (DHW)	TOTAL
			MIINERGIE simple flux	SIA 380/1	
	[m <sup>2</sup> ]		[kWh/yr]	[kWh/yr]	[kWh/yr]
1	8'200	273	245'180	170'833	416'013
2	2'615	76	82'308	50'104	132'412
3	2'415	70	76'328	45'938	122'266
4	2'780	92	83'122	57'917	141'039
5	3'700	116	113'246	74'306	187'552
6	1'500	50	44'850	31'250	76'100
7	2'870	83	90'652	54'653	145'305
8	2'500	83	74'750	52'083	126'833
9	4'225	140	126'328	88'021	214'349
10	4'455	148	133'205	92'813	226'018
11	4'190	139	125'281	87'292	212'573
12	2'300	76	68'770	47'917	116'687
13	2'300	76	68'770	47'917	116'687
14	2'300	76	68'770	47'917	116'687
<b>TOT</b>	<b>46'350</b>	<b>1'498</b>	<b>1'401'559</b>	<b>948'958</b>	<b>2'350'521</b>

The call for tender includes also information about the end use of the buildings, which is shown in Table 6. It can be seen that the buildings include, beside the residential use (multidwelling), also a small share of retail and restaurant services use, which are associated with different energy needs. Moreover, there is even a small indoor swimming pool, located in building one.

The energy profile of the buildings is calculated according to Minergie standard, as well as the SIA norms. Given the annual energy demand for space heating and hot water, as shown in Table 5, the monthly profile is shown in Figure 16.

#### 4.1.3 Pre-studies

Some pre-studies have been commissioned by the land-owner, in order to give, on an indicative basis, the sizing of the energy system. These studies have been realized by external engineering firms and the results are contained in the call for tender. The studied parameters include the sizing for heat pumps, geothermal wells, as well as PV, and are shown in Table 7. They estimate a PV potential on the building roofs of  $570kWp$ , and the need for an installed heating power of  $1'258kW$ , using 77 geothermal wells of an average length of  $271m$ .



Figure 15: Map of the planned Eglantine district

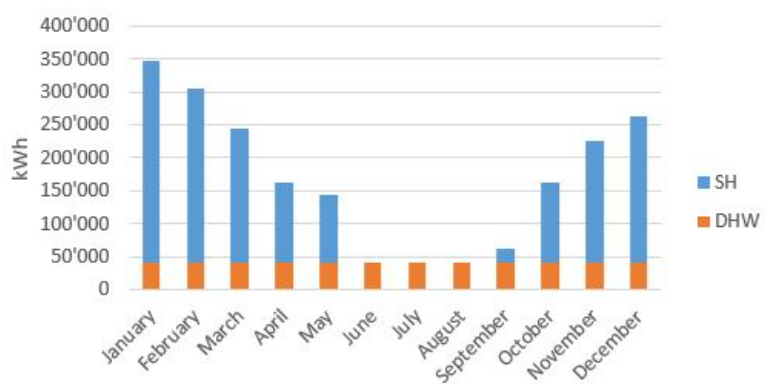


Figure 16: Annual energy distribution for space heating and hot water

Table 6: Estimated use of buildings in call for tender

<b>Building</b>	<b>Housing</b> [%]	<b>Retail</b> [%]	<b>Restaurant services</b> [%]	<b>Indoor swimming pool</b> [%]
<b>1</b>	89.58%	3.10%	4.42%	2.89%
<b>2</b>	97.54%	2.46%	0.00%	0.00%
<b>3</b>	100.00%	0.00%	0.00%	0.00%
<b>4</b>	100.00%	0.00%	0.00%	0.00%
<b>5</b>	93.19%	6.81%	0.00%	0.00%
<b>6</b>	95.79%	4.21%	0.00%	0.00%
<b>7</b>	95.79%	4.21%	0.00%	0.00%
<b>8</b>	100.00%	0.00%	0.00%	0.00%
<b>9</b>	100.00%	0.00%	0.00%	0.00%
<b>10</b>	100.00%	0.00%	0.00%	0.00%
<b>11</b>	100.00%	0.00%	0.00%	0.00%
<b>12</b>	100.00%	0.00%	0.00%	0.00%
<b>13</b>	100.00%	0.00%	0.00%	0.00%
<b>14</b>	100.00%	0.00%	0.00%	0.00%
<b>Tot</b>	97.08 %	1.63 %	0.78 %	0.51 %

Table 7: Estimated sizing of energy system in call for tender

<b>Building</b>	<b>HP</b>	<b>PV</b>	<b>Geothermal</b>	
	[kW]	[kWp]	Nb. wells	Depth [m]
1	46	223	13	284
2	45	70	4	291
3	35	64	4	269
4	33	76	5	250
5	49	100	6	276
6	55	41	3	225
7	55	77	5	256
8	37	68	4	281
9	66	115	7	271
10	0	121	7	286
11	59	114	7	269
12	33	63	4	259
13	32	63	4	259
14	27	63	4	267
<b>TOT</b>	<b>570</b>	<b>1'258</b>	<b>77</b>	

#### 4.1.4 Calculations/Energy demand/Typical days

- typical days resulting profile
- cooling demand deduced from SIA or minergie
- ...

write section eglantine calculations/energy demand

Figure 17, including occurrences.

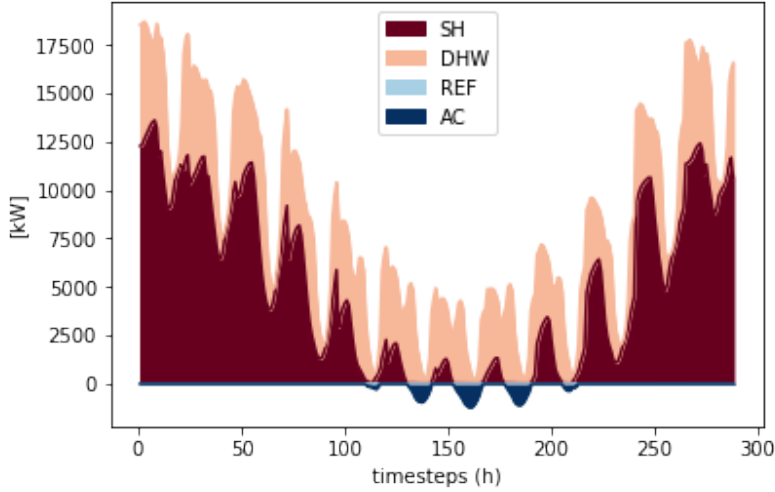


Figure 17: Total energy demand of the Eglantine district

## 4.2 Heat sources

The heat pumps in a system can source heat from various sources. Depending on the case, it is more convenient to use one or the other, given the varying temperatures and investment costs.

### 4.2.1 Stream

A small stream flows along the eastern boundary of the area, on which the Eglantine district is being built. The official numbers of the canton Vaud [?] are shown in Figure 18, in which the Temperature and the water flow are plotted. These values represent the average over a period of several years (7 for the temperature, and 12 for the flow rates).

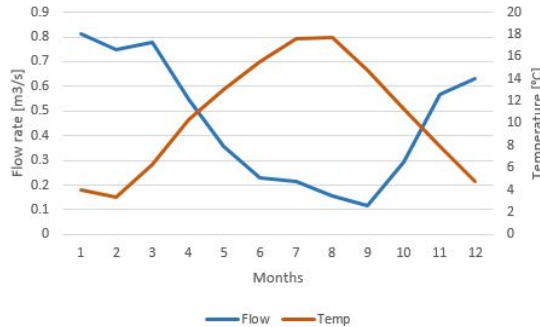


Figure 18: Temperature and flow of the Morges river

According to this graph, it could be thought of using this river as a heat source for the heat pumps. However, what is not displayed is the minimum values. In fact, during droughts, the flow rate would not be sufficient to cover the heating/cooling demand. In fact, the lowest value has been reached in August 2004 with  $0.017\text{m}^3/\text{s}$ , and even in December 2005 the lowest daily flow was of  $0.057\text{m}^3/\text{s}$ .

For this reason, the stream has been excluded from further analysis and has not been considered as a viable solution.

### 4.2.2 Lake

Through a pipe, the water is pumped from the lake, at a depth of around 70 m, to the central plant, located in the district area.

The massflow of the water is calculated in order to satisfy a drop/rise in the water stream of  $\Delta T_{water} = 4^\circ\text{C}$ .

The cost function is calculated as for the CO<sub>2</sub> pipes (see Section 3.6.7), considering the needed diameter to satisfy the heating/cooling demand, which depend on the different heat capacity and massflow of the water.

#### 4.2.3 Geothermal wells

The average temperature of a geothermal well is calculated according to Section 3.2. The temperature gradient in the lemanic region is found in experimental data from the canton Geneva[?]:

$$\nabla T_g = 0.03[\text{K}/\text{m}] \quad (55)$$

This value also corresponds to the average gradient found in the Swiss plateau[?].

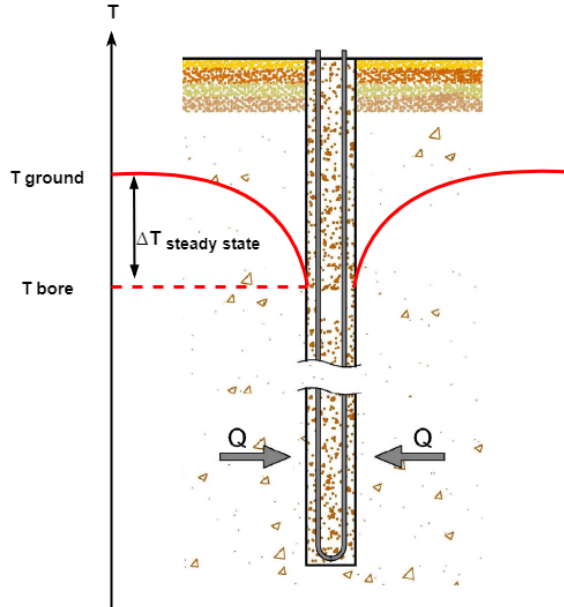
The average surface temperature depends mainly on the latitude and on the altitude. Standard values for different regions of Switzerland can be found in the SIA norm 384[?]. Experimental measurements[?] show that the surface temperature in the lemanic region is:

$$T_{g,s} = 11^\circ\text{C} \quad (56)$$

Knowing the average depth of the geothermal wells, which is found to be  $L_{gtw} = 267$  (see Section 4.1), the mean temperature in the geothermal well corresponds to:

$$T_{g,mean} = 15^\circ\text{C} \quad (57)$$

It is assumed that the geothermal wells are well sized, in order to respect the natural recharge rate, which is strongly dependent on the type of soil. The sizing of the boreholes is very important to ensure a sustainable use of the ground heat throughout the years.



add images  
of gradient  
and surface  
temperature  
from PGG  
report?

Figure 19: Steady state temperature difference in borehole, due to heat extraction

Nevertheless, there is a temperature gradient that will form around the borehole at any time heat is extracted, as shown in Figure 19, in the steady state that depends of the heat extraction rate and the conductivity of the soil. It has to be noted that this temperature gradient would be positive during heat dissipation. However, this is not in the scope of this work and it has been chosen to assume a negative temperature difference ( $\Delta T_{steady state}$ ) of  $3^\circ\text{C}$  [?, ?], due to the

reduced cooling demand for this application. Thus the mean useful temperature of the borehole over its depth is given by:

$$T_{b,mean} = T_{g,mean} - \Delta T_{SteadyState} = 12^\circ\text{C} \quad (58)$$

The minimum approach temperature necessary to exchange heat with the soil can be determined with help of the procedure described in Section 3.4.

The price for boreholes in Switzerland is found to be around  $80\text{CHF/m}$  [?]. Assuming a typical pipe diameter of  $32\text{mm}$ [?, ?], the corresponding cost of the heat exchange area of the borehole calculated.

To perform the  $\Delta T_{min}$  optimization, the overall heat transfer coefficients of the well - including the fluid, the bore wall and the soil - are assumed to be[?]:

$$U^{g/water} = 9.3\text{kW/m}^2\text{K} \quad U^{g/CO2} = 17.1\text{kW/m}^2\text{K} \quad (59)$$

The resulting minimum approach temperatures in ground heat exchanges are:

$$\Delta T_{min}^{g/water} = 14^\circ\text{C} \quad \Delta T_{min}^{g/CO2} = 6.8^\circ\text{C} \quad (60)$$

These values are similar to experimental or standard values found in literature [?, ?].

The water rise/drop in the water ground loop is assumed to be  $dT_{water} = 4^\circ\text{C}$  [?]

The price for boreholes in Switzerland is found to be around  $c_{wells} = 80$  [CHF/m] [?]. In order to provide the model with an energy dependent cost function, this value is transformed with help of the data from Table 7:

$$L_{wells}^{tot} = n_{wells} * L_{well}^{average} \quad (61)$$

$$\text{Cost function [CHF/kW]} = c_{wells} \frac{L_{wells}^{tot}}{P_{hp}^{tot}} \quad (62)$$

this cost  
function  
here?

where  $L_{wells}$  is the length and  $n_{wells}$  the number of boreholes, and  $P_{hp}$  is the total power of heat pumps installed.

inv cost is given by the Qwinter-Qsummer

### 4.3 External heat sources

The main advantage of a 5th generation district heating network is the ability to recover heat, and exchange it among the diversity of user. In the case of the Eglantine project, inside the district there are only very small heat sources and it is thus necessary to identify potential heat sources, located in the surroundings. Two potential heat sources have been identified in the surroundings of the Eglantine district: the ice rink and a shopping mall.

#### 4.3.1 Ice rink

An ice rink is a place where people can ice skate and play winter sports. The ice surface is normally inside an arena, which ensures comfortable temperatures for the people on the ice, as well as for the public, throughout the season. This also allows to extend the season, avoiding ice melt, when temperatures are warmer outside.

A study, conducted on more than one hundred ice rinks in Sweden, shows that the refrigeration system used to cool the ice surface has the largest share in total energy consumption, 43% (in average) as indicated in Figure 21 [?]. However, the ice rink often also includes changing rooms with showers, and a cafeteria or a restaurant, which also present heating demand. According to Figure 21, the average share of heating in the total energy demand is 26%. Last but not least, the ice surface has to be constantly illuminated, which requires a powerful lightning system. The

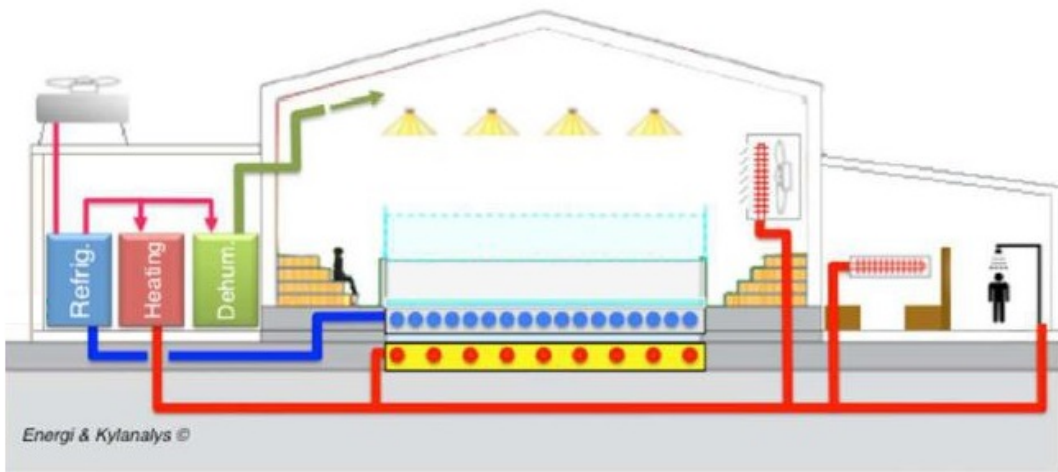


Figure 20: Energy system of a typical ice rink [?]

global system is shown in Figure 20.

However, for practicality reasons, it is assumed that only the refrigeration system is connected to the CO<sub>2</sub> network, while the heating and electricity demand is supplied by the existing system, and are thus not considered in this model.

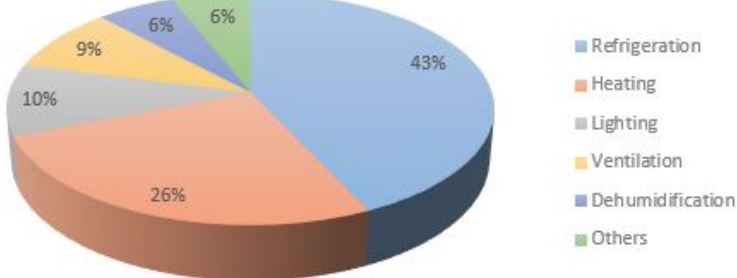


Figure 21: Energy demand of a typical ice rink [?]

Ice rinks are conventionally cooled with indirect systems, as shown in the right part of Figure 22, based on a ammonia (NH<sub>3</sub>) vapor compression chiller, exchanging with a secondary brine loop that extracts the heat from the ice surface. The waste heat is normally, or at least in older systems, exchanged with the environment, with help of cooling towers. Connecting it to a 5th generation district heating network, would allow recovering this heat and use it to cover the heat demand of other users. The connection to the CO<sub>2</sub> network is shown in the left part of Figure 22.

This presents a high energy and exergy efficiency gain, since the refrigeration system can be driven on a lower and constant condensation temperature.

The calculation of the cooling demand of the ice rink is based on the following assumptions:

- Constant load profile throughout the ice season
- Ice season: 1st of August - 1st of April
- $COP_{ref} = 4$  [?]

insert equations for temperatures with  $dT_{mins}$ ?

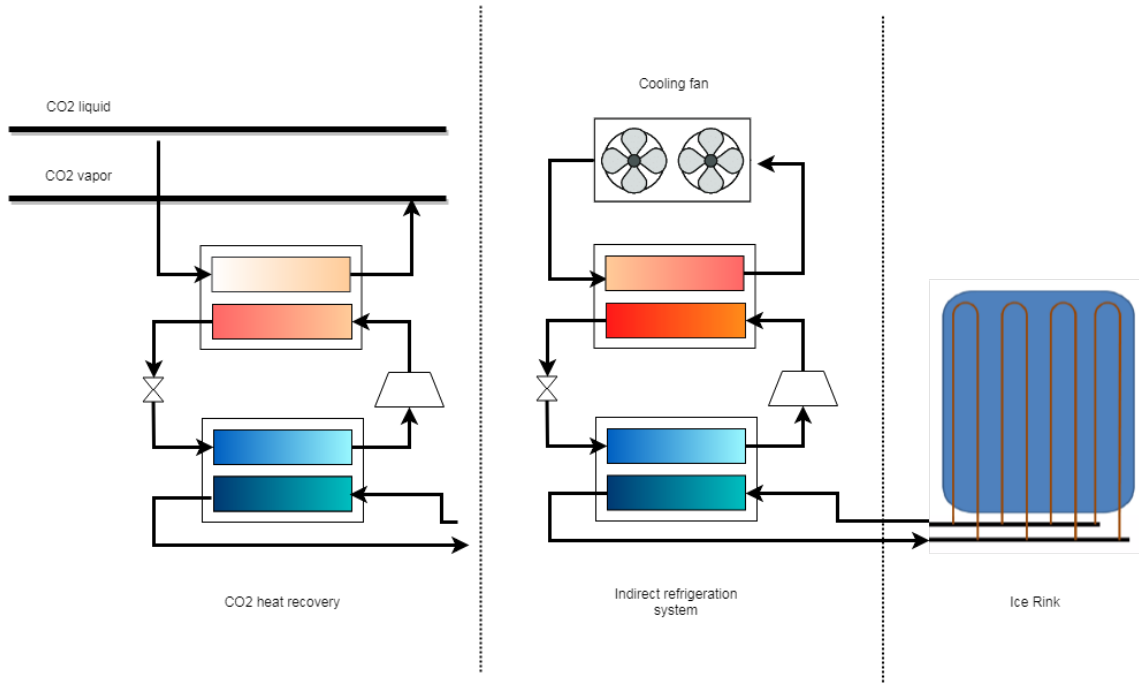


Figure 22: Refrigeration systems for ice rinks

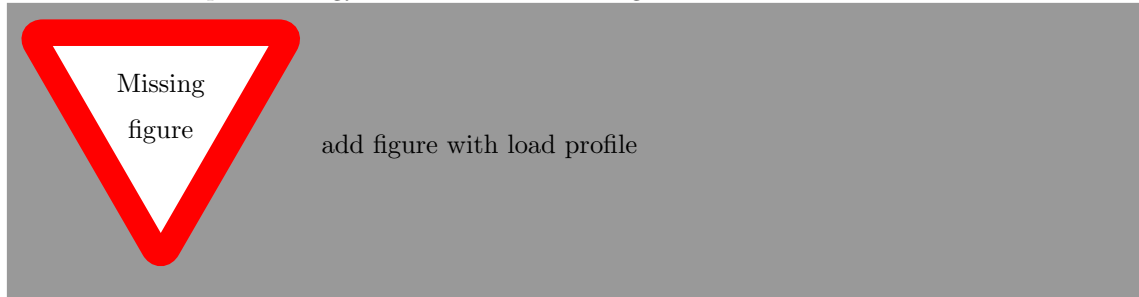
- Total waste heat =  $450\text{MWh/year}$  [?]
- $dT_{min}(\text{refrigerant} - \text{ice}) = 1^\circ\text{C}$
- $dT_{min}(\text{refrigerant} - \text{refrigerant}) = 3^\circ\text{C}$

The daily cooling demand profile of the ice rink, is based on the required ice temperature, which varies throughout the day[?], as shown in Table 4.3.1.

Table 8: Ice rink refrigeration profile

Period	Rink function	$T_{ice}$ [ $^\circ\text{C}$ ]
0.00-6:00	Night setback	-1
6:00-8:00	Ice maintenance	-1
8:00-16:00	Low load	-3
16:00-18:00	Figure skating	-4
18:00-24:00	Hockey	-6

Thus the computed energy demand is shown in Figure...



The refrigeration system is modeled the same way as in the reference scenario, taking the lower heat delivery temperatures into account.

### 4.3.2 Shopping mall

## 4.4 Variants / Scenarios

### 4.4.1 Heating

The heating demand is supplied by a set of decentralized geothermal heat pumps, one for domestic hot water and one for space heating in every building. These heat pumps source the ambient heat from a secondary loop that exchanges heat with the ground through a system of geothermal wells, the SL-GSHP, which is described in Section 2.4.

Given the relevance of the heat pumps in the studied energy system, it has been chosen to use its thermodynamic model, which achieves more reliable and precise results.

The temperatures at the evaporator and condenser are given by the following equations:

$$T_{evap} = T_{ground} - \Delta T_{min}^{ground/water} - \Delta T_{water} - \Delta T_{min}^{ref/water} \quad (63)$$

$$T_{cond} = T_{demand} + \Delta T_{min}^{ref/water} \quad (64)$$

where  $\Delta T_{min}$  are the corresponding minimum approach temperatures, and  $\Delta T_{water}$  is the temperature rise in the secondary water loop exchanging with the ground.

For the space heating heat pump, the refrigerant used is R123yf, as described in Section 3.6.2.

For the domestic hot water, it is chosen to use transcritical CO<sub>2</sub> heat pumps. As described in Section 3.6.3, this technology can achieve very good performances supplying heat that requires a high lift. This is the case in domestic hot water, where the water has to be heated from a temperature of 10 °C to a temperature of 55 °C.

### 4.4.2 Cooling

Given the availability of geothermal wells, it has been chosen to implement geo-cooling for space cooling. The system is providing cooling at the ground temperature, corrected with the minimum approach temperature  $\Delta T_{min,ground/water}$  and the temperature rise in the water loop  $\Delta T_{water}$ .

$$T_{geo-cooling} = T_{ground} + \Delta T_{min}^{ground/water} + \Delta T_{water} \quad (65)$$

### 4.4.3 Refrigeration

The refrigeration is achieved with a set of decentralized air cooled vapor compression chillers, which present the same working principle as heat pumps. Given that energy demand for refrigeration is not as relevant in the case study, it has been chosen to use the basic Carnot cycle model, as explained in Section 3.6.1. The heat is evacuated into the environment with help of cooling towers, as described in Section 3.6.4.

Thus, the total energy consumption is a sum of the energy demand of the compressor and the cooling fans.

$$\dot{E} = \dot{E}_{ref} + \dot{E}_{fans} \quad (66)$$

and the operating temperatures are defined in the following way:

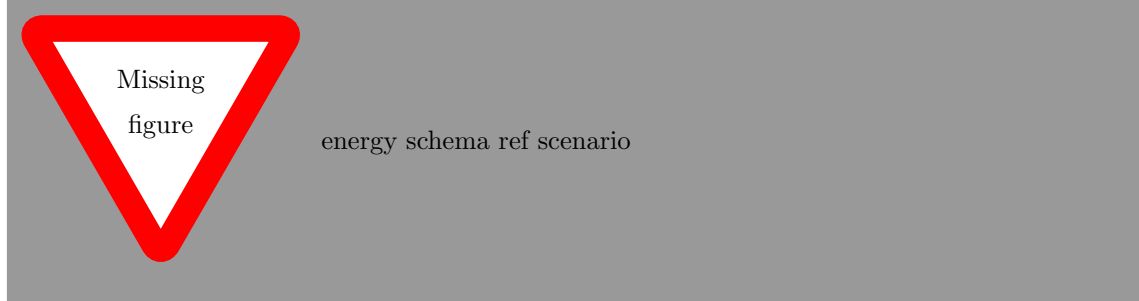
$$T_{cond} = T_{ext} + \Delta T_{air} + \Delta T_{min}^{ref/air} \quad (67)$$

where  $\Delta T_{air}$  is the temperature difference of the cooling air between the input and the output of the condenser, while  $\Delta T_{min}^{ref/air}$  is the minimum approach temperature difference needed for heat transfer between a refrigerant and air.

## 4.5 Reference scenario

In order to evaluate the potential of alternative energy systems, a reference scenario is defined. Data about the energy system that will be built in the Eglantine district is not available to the author, and therefore a standard state of the art system is used. It is assumed that the heat demand for space heating and domestic hot water is provided by decentralized geothermal sourced heat pumps. The cooling demand is provided by air cooled vapor

chillers, also commonly known as air conditioners. The scenario foresees the installation of PV panels on the roof of the buildings.



The main resource flows are shown in Table 9.

Table 9: Resource flows for the reference energy system ((-): flow in / (+): flow out))

Units	Electricity	Resource flows	
		$Source_{hot}$	$Source_{cold}$
$HP_{sh}$	-	-	+
$HP_{dhw}$	-	-	+
$HP_{ref}$	-	+	-
$HE_{ac}$		+	-
Elec. Heater	-		
PV	+		
$GTW_{winter}$		+	-
$GTW_{summer}$		-	+

### 4.5.1 Heating

The heating demand is supplied by a set of decentralized geothermal heat pumps, one for domestic hot water and one for space heating in every building. These heat pumps source the ambient heat from a secondary loop that exchanges heat with the ground through a system of geothermal wells, the SL-GSHP, which is described in Section 2.4.

Given the relevance of the heat pumps in the studied energy system, it has been chosen to use its thermodynamic model, which achieves more reliable and precise results.

The temperatures at the evaporator and condenser are given by the following equations:

$$T_{evap} = T_{ground} - \Delta T_{min}^{ground/water} - \Delta T_{water} - \Delta T_{min}^{ref/water} \quad (68)$$

$$T_{cond} = T_{demand} + \Delta T_{min}^{ref/water} \quad (69)$$

where  $\Delta T_{min}$  are the corresponding minimum approach temperatures, and  $\Delta T_{water}$  is the temperature rise in the secondary water loop exchanging with the ground.

For the space heating heat pump, the refrigerant used is R123yf, as described in Section 3.6.2.

For the domestic hot water, it is chosen to use transcritical CO<sub>2</sub> heat pumps. As described in Section 3.6.3, this technology can achieve very good performances supplying heat that requires

a high lift. This is the case in domestic hot water, where the water has to be heated from a temperature of 10 °C to a temperature of 55 °C.

#### 4.5.2 Cooling

Given the availability of geothermal wells, it has been chosen to implement geo-cooling for space cooling. The system is providing cooling at the ground temperature, corrected with the minimum approach temperature  $\Delta T_{min,ground/water}$  and the temperature rise in the water loop  $\Delta T_{water}$ .

$$T_{geo-cooling} = T_{ground} + \Delta T_{min}^{ground/water} + \Delta T_{water} \quad (70)$$

#### 4.5.3 Refrigeration

The refrigeration is achieved with a set of decentralized air cooled vapor compression chillers, which present the same working principle as heat pumps. Given that energy demand for refrigeration is not as relevant in the case study, it has been chosen to use the basic Carnot cycle model, as explained in Section 3.6.1. The heat is evacuated into the environment with help of cooling towers, as described in Section 3.6.4.

Thus, the total energy consumption is a sum of the energy demand of the compressor and the cooling fans.

$$\dot{E} = \dot{E}_{ref} + \dot{E}_{fans} \quad (71)$$

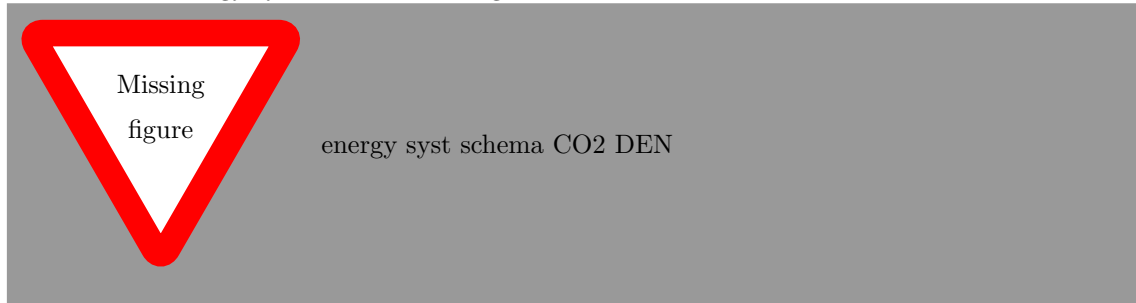
and the operating temperatures are defined in the following way:

$$T_{cond} = T_{ext} + \Delta T_{air} + \Delta T_{min}^{ref/air} \quad (72)$$

where  $\Delta T_{air}$  is the temperature difference of the cooling air between the input and the output of the condenser, while  $\Delta T_{min}^{ref/air}$  is the minimum approach temperature difference needed for heat transfer between a refrigerant and air.

### 4.6 CO2 DEN

CO2 network energy system showed in Figure...



The main resource flows are shown in Table 10.

#### 4.6.1 Heating

For space heating and domestic hot water, the same model as for the heat pumps in reference scenario are used. Since in this case the HP sources heat from the CO2 network instead of the geothermal wells, the major difference lies in the evaporation temperature, which corresponds to temperature in the CO2 vapor pipe ( $T_{CO2,g}$ ):

$$T_{evap} = T_{CO2,g} - \Delta T_{min}^{ref/ref} \quad (73)$$

Table 10: Resource flows for the CO2 DEN ((-): flow in / (+): flow out))

Units	Electricity	Resource flows			
		$CO2_{liq}$	$CO2_{vap}$	$Source_{hot}$	$Source_{cold}$
$HP_{cp}^{winter}$	-	-	+	-	+
$HP_{cp}^{summer}$		+	-	+	-
$HP_{sh}$	-	+	-		
$HP_{dhw}$	-	+	-		
$HP_{ref}$	-	-	+		
$HE_{ac}$		-	+		
Elec. Heater	-				
PV	+				
$GTW_{winter}$				+	-
$GTW_{summer}$				-	+

#### 4.6.2 Refrigeration

As for the reference scenario, refrigeration is achieved through decentralized vapor compression chillers. However, in this case they are not air cooled, but they exchange directly with the CO2 network. Thus, the temperature in the condenser is given by:

$$T_{cond} = T_{CO2,l} + \Delta T_{min}^{ref/CO2} \quad (74)$$

#### 4.6.3 Cooling

Free cooling has been modeled by a simple heat exchanger that evaporates saturated liquid CO2, which is then injected back into the network in a superheated vapor state with  $\Delta T_{superheating} = 1K$ . The mass flow of the CO2 is adapted to satisfy the cooling demand. It is assumed that pressure and temperature losses are negligible.

#### 4.6.4 Central plant

As mentioned before, for obvious reasons, heating and cooling loads in the system are not always balanced. Thus, there is the need for a central plant to balance out the system, able to heat and cool. A centralized heat pump is very suitable for this purpose.

Equations and modeling are the same as for the above described heat pumps. Difference consists in heat source, and thus evaporation temperature. Different options have been studied:

- River: as for the lake, river water can be an interesting source of heat, with the difference of seasonal fluctuations. During the winter, river water can have a temperature close to 0, while in the summer it can rise to more than 20 °C. In the case of the Eglantine district, there is a small stream, called Morges, that passes at the eastern border of the land.
- Lake: sourced from a certain depth, lake water shows an almost constant temperature of around 7.5 °C throughout the year. This solution can be very interesting alternative to geothermal wells, since, if close enough, it might reduce the upfront costs, despite probably slightly increasing the operating costs. In this particular case, the distance to the lake is of 1500 m.
- Geothermal wells: after a certain depth, the ground presents a constant and very interesting temperature throughout the year. This heat can be exchanged with help of a secondary loop or through direct expansion of the refrigerant into the ground coils.

Direct expansion system is assumed (see Section 2.4). So the CO2 DEN with DX-GSHP technology is shown in Figure 23

The operating temperatures are calculating the following way.

explain  
lake=ref,  
geoth=DHX  
CO2

$$T_{evap} = T_{source} - \Delta T_{min}^{CO2/source} \quad (75)$$

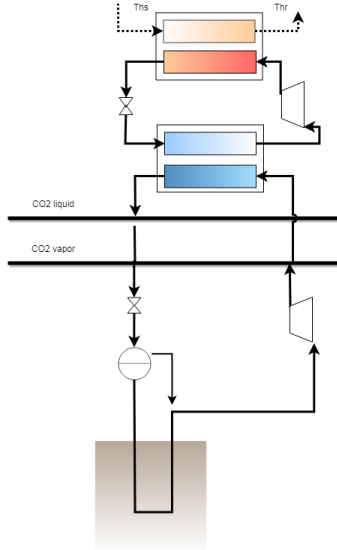


Figure 23: A simplified schematics of the CO2 DEN with DX-GSHP technology

The operating pressure is calculated with help of *Coolprop*. The results are shown in Table 11.

Table 11: Operating conditions for direct expansion of CO<sub>2</sub> in heat source

Source	$\Delta T_{min}^{ref/source}$ [°C]	$T_{source}$ [°C]	$T_{evap}$ [°C]	$P_{CO_2}$ [bar]
Lake	4	7.5	3.5	38.2
Geothermal	10	11	1	35.8

## 4.7 Values/typical days/...

- $c_{inv}$
- $c_{el-/+}$
- $cop$ : In this project,  $cop_1$  (fixed) value is assumed to be negligible.
- $d_{tmin}$
- with respectively 1 and 2 °C of superheating and subcooling at the outlet of the heat exchanger [ ].
- ...

### 4.7.1 Investment cost functions

As described in Section 2.6, the model need investment cost parameters that can be calculated with the procedure explained in Section 3.3.

Values for the heat pumps are given in Henchoz et al., obtained by linearizing commercial products[?]. The cost function for heat exchangers has been interpolated in order to have a function dependent on the amount of exchanged heat.

Values are summarized in Table 12.

summary table needed here ( $T_s$ ,  $dT_{min}$ ,  $T_{evap}$ ,  $P_{...}$ )?  
wrong values now

Table with values

missing reference for superheat and subcool temp

Table 12: Summary of the investment cost function of each technology, including their expected lifetime and the interest rate.

Technology	Cost function [Euro]	X [unit]	Interest rate	Lifetime
HP	$1'240 X + 5680$	$E_{comp}$ [kW]	0.08	20
heat exchanger	$215 X + 56$	$Q$ [kW]	0.08	20
Electric heater	$23 X + 968$	$Q$ [kW]	0.08	20
PV	$300 X$	$A$ [ $m^2$ ]	0.08	20
Geothermal wells	$2890 X + 5800$	$Q$ [kW]	0.03	50
Network	See Section 3.6.7			

#### 4.7.2 Minimum approach temperature

As seen in Table 3, CO<sub>2</sub> (R744) has a higher heat transfer coefficient than other conventional refrigerants, as for example R1234yf. This has to be taken into account in the energy system through a different minimum approach temperature. To do so, there are two possible approaches:

- calculate a new, lower,  $\Delta T_{min}^{R744}$ , maintaining the same heat exchange area  $A_{ex}$ . This results in higher COP for the heat pump and thus lower operating costs  $OC_{hp}$
- calculate a new, smaller, heat exchange area  $A_{ex}$ , maintaining the same  $\Delta T_{min}$ . This leads to lower upfront costs  $IC_{ex}$

It is chosen to use different  $\Delta T_{min}^{R744}$ , maintaining the same heat exchange area. The following procedure is repeated for the various fluids ( $X$ ) the refrigerants have to exchange with:

1. Calculate  $U_{R1234yf/X}$  with Equation 26
2. Optimize  $\Delta T_{min}^{R1234yf/X}$  with numerical values from the Eglantine district, as described in Section 3.4
3. Calculate  $U_{R744/X}$
4. Solve Equation 23 in function of  $\Delta T$ , using  $U_{R744/X}$  and the  $A_{ex}$  resulting from the previous step.

The implementation of this algorithm has been solved on *Matlab* with help of function *solve(equation 23,  $\Delta T_{min}$ )*. Thus resulting  $\Delta T_{min}$  values shown in Table 13.

Table 13: Minimum approach temperatures used for heat exchanges in the model

$\Delta T_{min}$ [K]	Ground	Water	R744	R1234yf
Water	14	-	-	-
R744	6.8	3.46	0.8	-
R1234yf	-	4	1.4	2.3

As example, Figure 24 and Figure 25 show the resulting optimization of the minimum approach temperatures, respectively for refrigerant and ground heat exchanges. The straight line shows the optimum  $\Delta T_{min}$  for the reference heat exchange, in function of the total costs (green line), while the dashed line shows the improved  $\Delta T_{min}$  for CO<sub>2</sub>, maintaining the same  $A_{ex}$ .

#### 4.7.3 Compressor efficiencies

The compressor efficiencies are directly calculated in the model, according to the equations in Section 3.6.3 and 3.6.2. could be directly implemented in model. Table 14 shows the resulting efficiencies in standard operating conditions, for the different heat pumps used in this work.

These values are similar to reference values found by Yang et al.[?] in their experimental work.

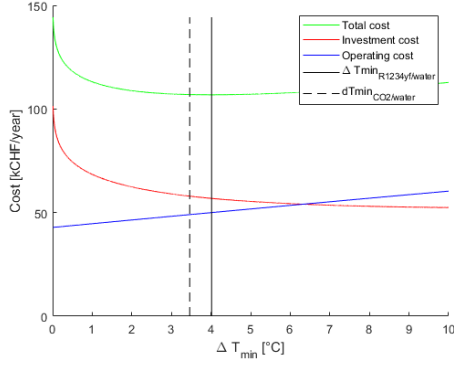


Figure 24: Optimization of  $\Delta T_{min}$  values for heat exchange with refrigerant R1234yf, through minimization of total costs (green line)

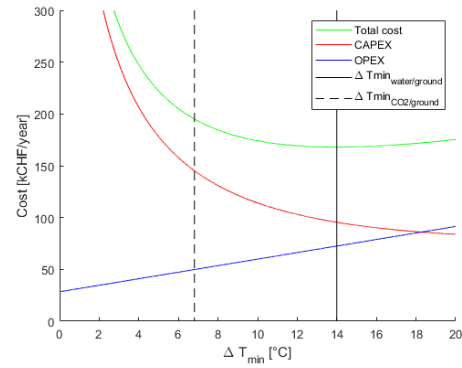


Figure 25: Optimization of  $\Delta T_{min}$  values for heat exchange with the ground, through minimization of total costs (green line)

Table 14: Calculated efficiencies for heat pump compressors

Unit Refrigerant	CO2 DEN					Reference scenario		
	CP R123yf	CP CO2	SH R123yf	DHW R744	REF R123yf	SH R123yf	DHW R744	REF R123yf
$P_d$	5.0	43.0	9.4	84.9	5.0	9.4	66.0	11
$P_s$	2.4	20.2	4.6	46.7	2.80	2.4	30.4	2.4
$\eta_{mech}$	0.85	0.80	0.85	0.78	0.85	0.85	0.80	0.85
$\eta_{is}$	0.85	0.70	0.85	0.71	0.85	0.82	0.70	0.81
$\eta_{comp}$	0.72	0.56	0.72	0.55	0.72	0.70	0.56	0.69

#### 4.8 CP with if conditions

In order to have a HP model for the central plant, which is able to handle different source temperatures, different cases have been implemented, with help of if conditions. Indeed, computation problems arise when the source temperatures reaches the condensation temperature of the heating part of the CP, which corresponds to the temperature of the CO2 network. In the same way, this higher source temperature also precludes the possibility of free-cooling. However, if the temperatures is higher than the CO2 network, the central pump might be able to source heat without operating a heat pump (free-heating).

not sure where to put that...

The model includes two operating modes for each part of the central plant, the heating part (CP-winter) and the cooling part (CP-summer). The thresholds are set in the following way:

$$T_{thresh}^{free-cooling} = T_{CO2} - \Delta T \quad (76)$$

$$T_{thresh}^{free-heating} = T_{CO2} + \Delta T \quad (77)$$

where  $\Delta T$  is the minimum temperature difference needed for the specific heat exchange.

The truth table is shown in Table 15.

The parameters that vary through the if conditions are the electricity consumed  $E_{cp}$  and the investment cost parameters.

#### 4.9 DX Vs. SL-GSHP

As discussed in Section 2.4, there is the possibility to directly expand the CO2 into the geothermal well, instead of exchanging with help of a secondary water loop. The different temperature levels are shown in Figure 26.

Results of simulation, show the difference in performance, 16.

Table 15: Truth table to determine if the CP operates in heat pump (HP) or in heat exchanger (HE) mode, depending on the borehole temperature and the threshold temperatures for free-cooling  $T^{FC}$  and free-heating  $T^{FH}$

$T_{borehole}$	$\leq T^{FC}$	$T^{FC} \leq T \leq T^{FH}$	$\geq T^{FH}$
CP-winter	HP	HP	HE
CP-summer	HE	HP	HP

Table 16: Comparison of simulation results for a SL-GSHP, versus a DX-GSHP

	SL-GSHP R1234yf	DX-GSHP R744
$T_{source}^{lm}$	12	12
$T_{demand}^{lm}$	15	15
$T_{cond}^{lm}$	16.4	15.8
$T_{evap}^{lm}$	-9.4	5.2
$COP_{real}$	6.5	15.8
$\eta_{COP}$	65 %	60 %

CO<sub>2</sub> heat pump has lower efficiencies (see Table 14) thus  $\eta_{COP}$  but much lower temperature difference to cover. Thus, its real coefficient of performance, as well as the exergy efficiency, are clearly higher than for the SL-GSHP. In fact, the DX-GSHP results being about twice as good.

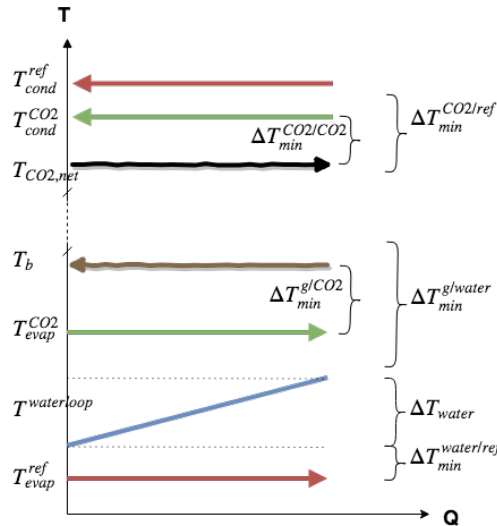


Figure 26: Schematic representation of heat exchanges and minimum approach temperatures for the central plant HP, comparing SL- and DX-GSHP

It has to be noted that this specific heat pump globally presents very low exergy values. This is due to ratio between the relatively high minimum approach temperatures and the very low temperature difference between the source temperature  $T_b$  and the heat demand temperature  $T_{vap}^{CO2}$ .

#### 4.10 Model improvement - thermodyn cycle

Comparison of results with simple Carnot model and with thermodyn model. Show difference in COPs

do i maintain results with simple cycles somewhere in the results to show how much better it is with cycle?

Recalculation of  $\eta_{COP}$  for all ETs. From the real COP calculated with help of coolprop and the thermodynamic cycle of the heat pump, the COP efficiency can easily be calculated

$$\eta_{COP} = \frac{COP_{real}}{COP_{theoretical}} \quad (78)$$

Table with new eta cop values.

COP Comparison with values from literature?

## 5 Results and discussion

### 5.1 Energy and exergy performance

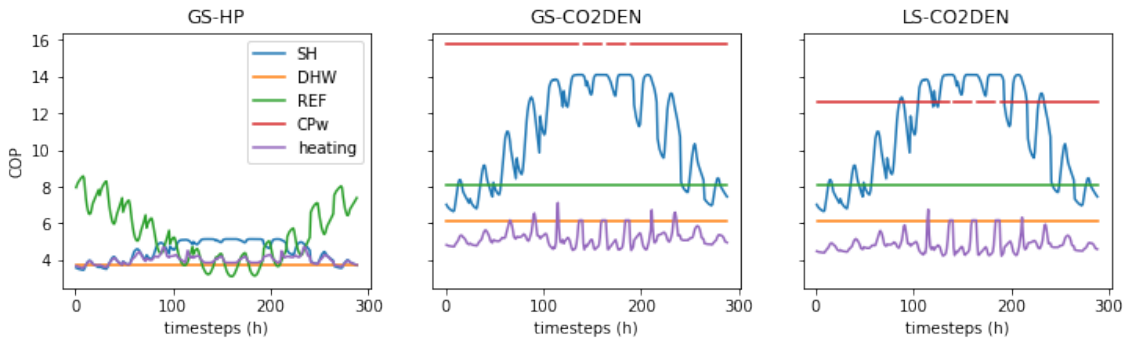


Figure 27: Comparison of COP values for each timestep  $t$  and unit. The *cooling* and the *global* COP are not displayed for practicality reasons, given their very high values during free cooling

A direct way to compare the performance of the different conversion technologies is the coefficient of performance, which is simply given by the ratio between the delivered heat  $Q$  and the consumed electricity  $E$ . If the temperatures of evaporation and condensation of a heat pump are fixed, the operating cycle is also fixed, and thus the COP value. However, modern HP can adapt the operating cycle to fit the varying heat demand temperature. This allows to strongly improve the COP, as well as the exergy efficiency. The COP values, calculated in each timestep, are shown in Figure 27. The heating heat pumps for SH and DHW are considerably higher in the CO2DEN. This is due to the "two stages" of the conversion technology: the heat is first furnished to the CO2 network by the CP and then brought up to the required temperature by the decentralized HP. The COP of the central plant is higher in the GS CO2DEN, being the evaporation temperature higher than in the heat exchange with the lake. The SH HP has COP that varies between 6 and 14. This is due to the fact that the temperature of the heat demand rises with the amount of heat required. Thus the COP of the HP is lower during winter. Moreover, the compression chillers in the GS-HP perform worse during summer, when they have to deliver heat to a higher ambient temperature, while the COP of refrigeration in the CO2DEN are constant, since heat is delivered the whole year to the CO2 network, which has at constant temperature.

The mean COP values for each technology are shown in Table 17. The GS-CO2DEN shows the best performance with a global COP of 6.1. The LS-CO2DEN follows with 5.6 and the GS-HP with 4.6. All the conversion technologies perform well, but the combination of the DX-GSHP central plant with the decentralized HP in the GS-CO2DEN obtains excellent results.

The exergy values of supply and demand have been calculated for each conversion technology, as explained in Section 3.5. This analysis shows the real thermodynamic value of the required energy services, since not only the amount of heat is considered, but also the temperature level at which it happens. The exergy value of the demand is thus calculated in function of the varying

Table 17: COP values for the three technological variants of energy system

	GSHP	GS-CO2DEN	LS-CO2DEN
HP-SH	4.5	10.8	10.8
HP-DHW	3.8	6.2	6.2
HP-REF	5.4	8.1	8.1
HP- $CP_{winter}$	-	15.8	12.6
Heating	4.0	5.2	4.9
Cooling	19.1	50.4	50.4
Global	4.6	6.1	5.6

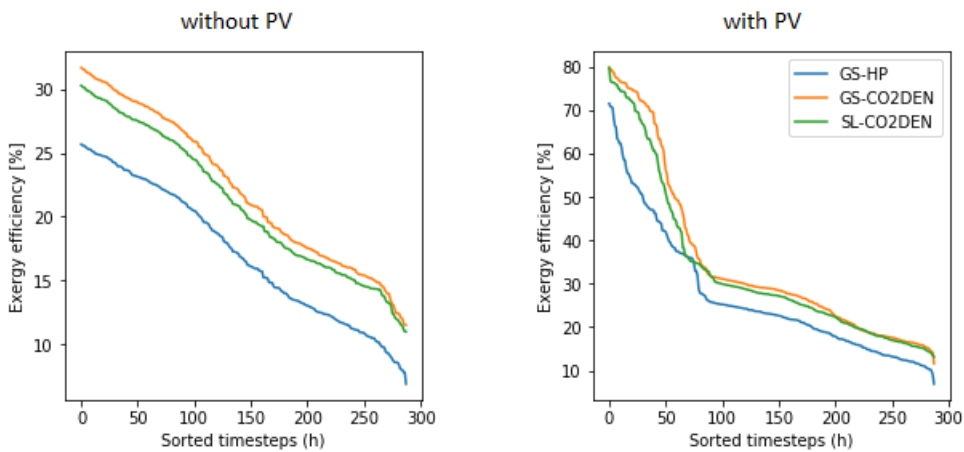


Figure 28: Comparison of exergy efficiencies calculated in each timestep - sorted in decreasing order - with the entire electricity demand on the left, and only with electricity bought from the grid on the right

ambient temperature and is the same for all technologies.

The difference in the exergy efficiency between the different conversion technologies is shown in Figure 28. On the left hand, the values are calculated without taking into account the domestic PV production of renewable electricity, while on the right hand this has been included in the calculation. It is clear to see that the GS-HP performs worse than the CO2 DEN. The average exergy efficiency is of 17%, against 35% of the GS-CO2DEN. As it can be seen in Table 18, the exergy losses  $\dot{L}_{\Delta T_{min}}$  due to the minimum approach temperature between the heat demand and the supply are small compared to the exergy losses occurring in the heat pumps  $\dot{L}_{HP}$ . The latter accounts for the COP of the heat pumps, which is as well dependent from the approach temperature with their respective heat sources. This explains the lower exergy efficiency of the GS-HP, for which its heat pumps require a much lower evaporation temperature, as discussed previously.

Even if for obvious reasons the exergy efficiency is considerably higher including the domestic PV production, the difference in performance between the different technologies does not change. This is explained by the fact that the self consumption values are very similar, as it can be seen in Figure 29 in purple, and the increase of efficiency is thus shared among all technologies. In this case the average exergy efficiency for the GS-HP is 27%, against 35% and 33% for respectively the GS- and the LS-CO2DEN.

Table 18: Comparison of the exergy losses  $\dot{L}$  and efficiencies  $\eta_{exergy}$ , with and without considering renewable PV production

-	units	GS-HP	GS-CO2DEN	LS-CO2DEN
$L_{\Delta T_{min}}$	[MWh]	77	47	47
$L_{HP}$	[MWh]	355	242	281
$L_{tot}$	[MWh]	432	289	327
$\eta_{exergy}$	[%]	17%	22%	21%
$\eta_{PV}^{exergy}$	[%]	27%	35%	33%

## 5.2 Financial analysis

A financial analysis of the three conversion technologies is shown in Figure 29.

Given that in this work the cost of operation (OC) depend only from the consumed electricity (no consumption of gas or other resources), this is directly correlated to the global COP of the system. As seen above (see Table 17), GS-CO2DEN presents the highest coefficient of performance and thus also the lowest OC (dashed line), with 263'216[*Euro/yr*], and GS-HP the highest with 290'833[*Euro/yr*]. The LS-CO2DEN presents an OC of 270'728[*Euro/yr*].

The investment costs are shown more in detail in the clustered columns. It is easy to note that the GS-HP has much lower upfront costs (179'884[*Euro/yr*]) than the GS-CO2DEN solution (222'603[*Euro/yr*]). Indeed, the reduction in the cost of the HP - which is due to the higher COP values - is compensated by a higher cost for the geothermal wells and the additional cost of the CO2 network. The first also originates from the higher COP values, for which a larger share of energy will come from the source, and thus require a larger capacity installed. The latter is intrinsic to the CO2DEN system, that requires a physical network of CO2 pipes to connect all the user. In the SL-CO2DEN there are obviously no costs related to the geothermal wells, but the cost for the water pipes that allow the water to be brought to the CP. Given the actual distance of the Eglantine district from the lake, this solution leads to much higher upfront costs than the competing technologies (310'103[*Euro/yr*]).

Despite the lower OC for the CO2DEN technologies, the total cost is clearly following the tendency of the IC, which present a larger difference. The GS-HP ends up being the cheapest variant with 470'717[*Euro/yr*], followed by the GS-CO2DEN with an only slightly higher cost of

485'819 [Euro/yr]. The SL-CO2DEN is the most expensive solution with 580'0831 [Euro/yr].

Self consumption and autarchy do not vary much between the technologies, because no storage technology has been taken into account. Indeed, any kind of storage - thermal, electrical or CO<sub>2</sub> - would enable to adapt the consumption to profit from the cheap domestic produced energy, as well as to reduce peak demands. Moreover, despite of the optimizer choosing install the maximum possible amount of PV - which corresponds to the roof surface - for the three technologies, in order to reduce the OC, the amount of electricity produced is seldom larger than the total electricity demand of the district. Thus, the three systems have an autarchy of about 25 %, and a self consumption rate of around 75 %.

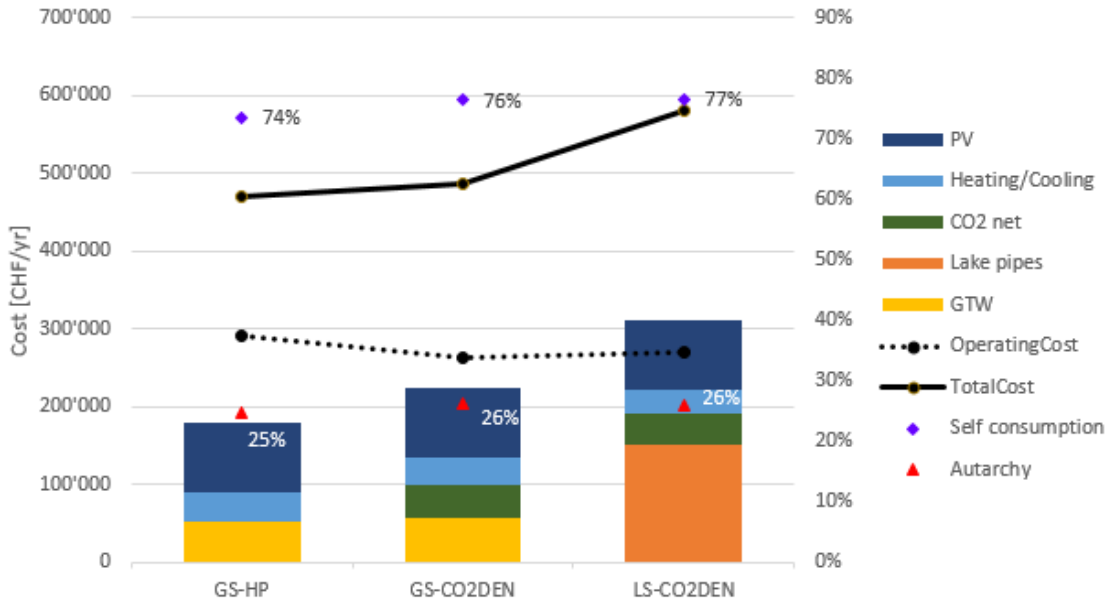


Figure 29: Cost comparison for the three different energy systems variants

### 5.2.1 Reference energy system

A parametric optimization of the costs of the reference energy system (GS-HP) is shown in Figure 30.

It can be seen that the biggest difference in investment and operating cost is due to the sizing of the PV. In fact, when constraining the investment costs, the model installs only a small share of PV, which increases the operational costs. On the contrary, a high share of PV increases the systems rate of auto-sufficiency, lowering the operational costs.

On the far right, the maximum allowed share of photovoltaic (PV) - set to twice the total roof area, which accounts for potential facades and free space PV - is reached. The operational are lowered thanks to a different handling of peak consumption. The optimal system installs a small share of electrical heater (R-EL) to cover peak demand, which allows to optimally size the heating heat pumps (HP-S, HP-DHW). In the last column on the right, the system chose not to install the electrical heater but installing larger heat pumps, which strongly increases upfront costs, but allows to further reduce the operational costs.

On the far left, the opposite phenomenon happens. To reduce upfront costs, the system chose to cover the heat demand almost entirely with help of the electric heater (R-EL), minimizing the size of the heating heat pumps (HP-SH, HP-DHW).

The optimum, with respect to the total cost of the energy system, is in the very middle of the graph, between column 2 and 3. The optimum is analyzed in the following chapters.

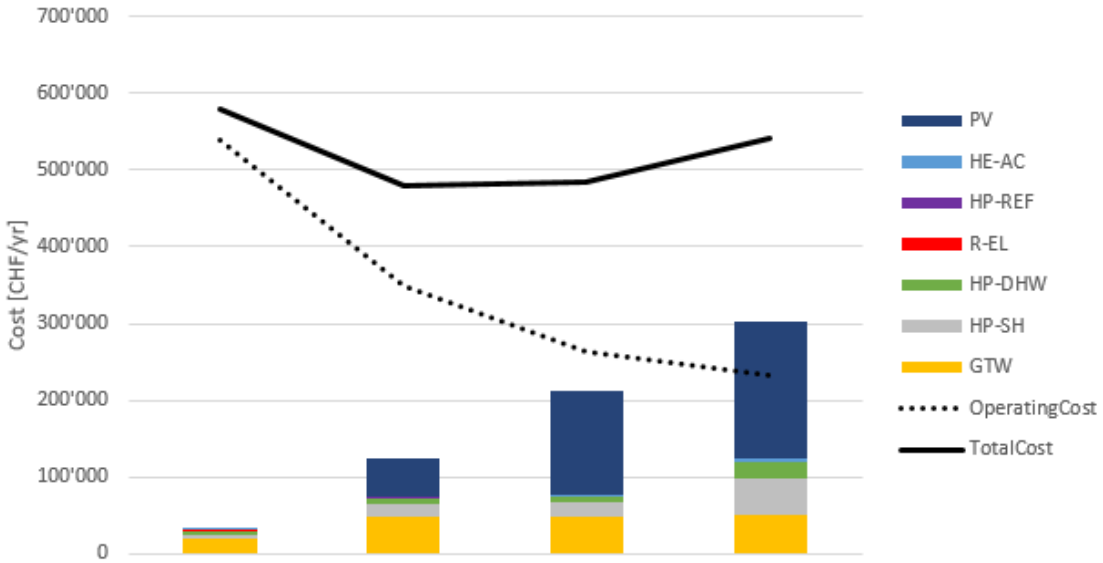


Figure 30: Parametric optimization of the reference energy system (GS-HP), showing the detailed investment costs, the operational cost and the total cost

### 5.2.2 CO2 DEN on geothermal wells

A parametric optimization of the costs of the CO2 district energy system with ground sourced central plant (GS-CO2DEN) is shown in Figure 32.

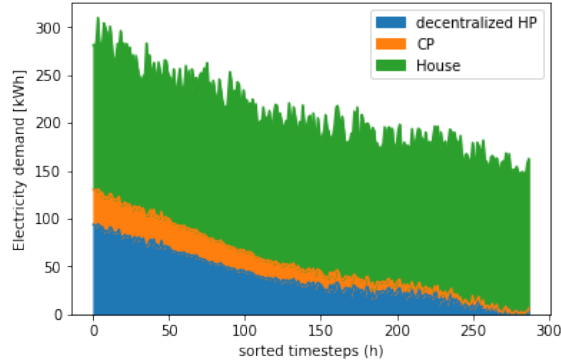


Figure 31: Electricity demand of GS-CO2DEN system grouped in categories, sorted in decreasing order

Ecp about 10 and 30% of Etot w and wo elhouse

The response of this system to the parametric optimization is very similar to the one of the GS-HP system. This means that the biggest difference in investment and operating cost is due to the sizing of the PV, while the extreme cases are determined by the ration between the electrical heater (R-EL) and the heating heat pumps (HP-SH, HP-DHW).

Also in this case the lowest total cost of the energy system is to be found in the very middle of the graph, between column 2 and 3. The optimum is analyzed in the following chapters.

If we take the stable middle, isolate PV costs we obtain a share of network and HP correposnding to... This is shown in Table 19, in comparison with existing anergy networks in Switzerland.

It can be seen that the GS-CO2DEN system in the Eglantine district presents a much lower percentage of the investment cost  $IC_{Heating/cooling}$  attributed to the heating and cooling equipment (HP-SH, HP-DHW, HP-REF, HE-AC) than two reference anergy networks in Switzerland.

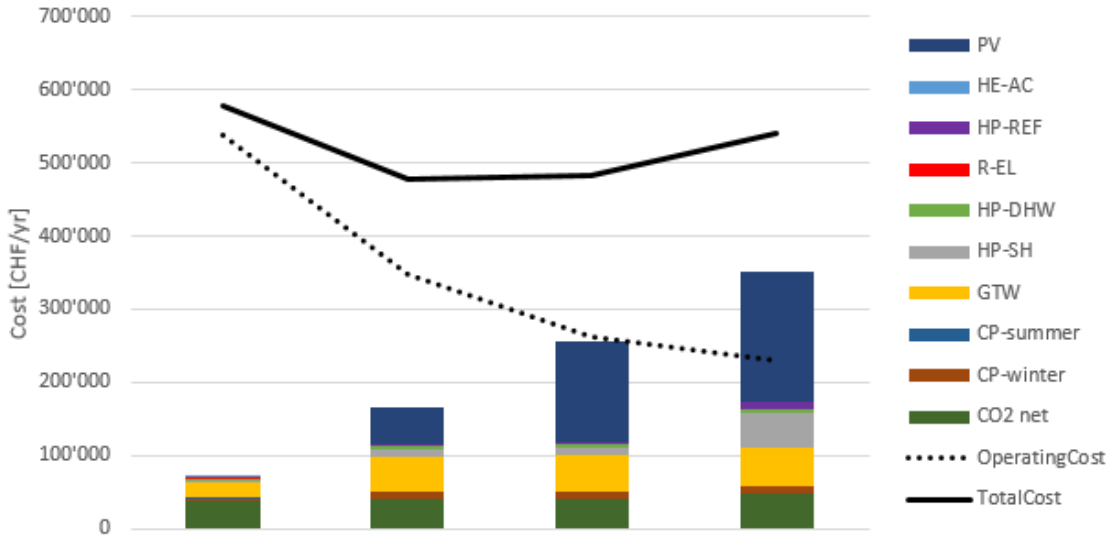


Figure 32: Parametric optimization of the ground sourced CO2 DEN (GS-CO2DEN), showing the detailed investment costs, the operational cost and the total cost

Table 19: Cost comparison with existing anergy systems

	Eglantine	Anergienetz ETH Hönggerberg	Anergienetz Friesenberg	
$IC_{NET}$	[%]	31.4 %	15.7 %	25.9 %
$IC_{GTW}$	[%]	42.0 %	32.7 %	23.5 %
$IC_{Heating/Cooling}$	[%]	26.5 %	49.2 %	50.6 %
Heating power	[kW]	592	8'000	3'930
Heating demand	[MWh/yr]	2'390	28'450	35'000
Cooling power	[kW]	84	6'000	3'500
Cooling demand	[MWh/yr]	33	26'200	80'000

One reason for this difference is most likely the size difference between the energy systems. In fact, the Eglantine system is drastically smaller than the one at ETH or in Friesenberg, which have a heating demand which is respectively 12 and 15 times bigger. The specific investment costs for building the network and drilling the geothermal wells decreases with size - for example the costs of digging to place a pipe underground won't be strongly correlated with the pipe diameter. On the contrary, the specific costs for the heat pumps will stay about the same, given that the size of the decentralized heat pumps will not increase, only its number.

On the other hand, it is not trivial to estimate the cost of building the CO<sub>2</sub> network, given the lack of examples in the real world, and the resulting costs could be proven to be inaccurate. Also the sizing of the geothermal well, in order to account for yearly energy balance and recharge rate, and for the specific cost, according to depth and soil type would have to be verified and confirmed through further studies and simulations.

### 5.3 Ground temperature

A critical parameter for the efficiency of a ground sourced energy system is the ground temperature. As seen in Section 3.2, this temperature depends mainly on the depth, the temperature gradient in the given soil and the surface temperature. In other words, it is dependent from the location - including local climate and altitude - and the depth of drilling. In order to acknowledge the influence this temperature has on the system's performance, a sensitivity analysis has been performed. The results are shown in Figure 33

The GS-HP energy system seems to responds in a linear way to the temperature raise, as it can be expected, thanks to the lower required temperature raise for heating, which increases the COP of the system. In reality a small step can be identified between 14 and 15 °C, at which the IC drop and the OC rise. This step happens when the ground is not cool enough anymore to offer the option of free-cooling. The system is forced to use a refrigeration system instead, which increases the OC. However this utility is already installed, and thus the increase of  $IC_{HP-REF}$  is lower than the reduction of the obsolete  $IC_{HE-AC}$ .

The GS-CO2DEN energy system presents a more evident step in its response to the ground temperature. The reason lies in the use of the central plant, which, as described in Section , has different operating modes for cooling and heating. In fact, if the temperatures are either high or low enough, it can operate free-cooling or free-heating. In any other case, it operates in cooling and/or heating HP mode. In this case the step happens at  $T_b \geq 16^\circ\text{C}$ , for which the CP can source heat directly from the ground without the need of a heat pump, which drastically reduces the operational costs.

For obvious reason, while GS-CO2DEN and GSHP respond similarly to the variation in the bore temperature, the LS-CO2DEN presents constant costs. In fact the system is not dependent from the ground temperature and is represented on the graph for sake of comparison. It can be seen that  $OC_{LS-CO2DEN}$  performs better, in terms of operating costs, than the GS-HP at any ground temperature in the studied interval. It also performs better than the GS-CO2DEN for temperatures below 10 °C. The lake distance in the Eglantine district is 1500m , which results in very high investment costs, precluding the competitiveness of this solution, in the given conditions.

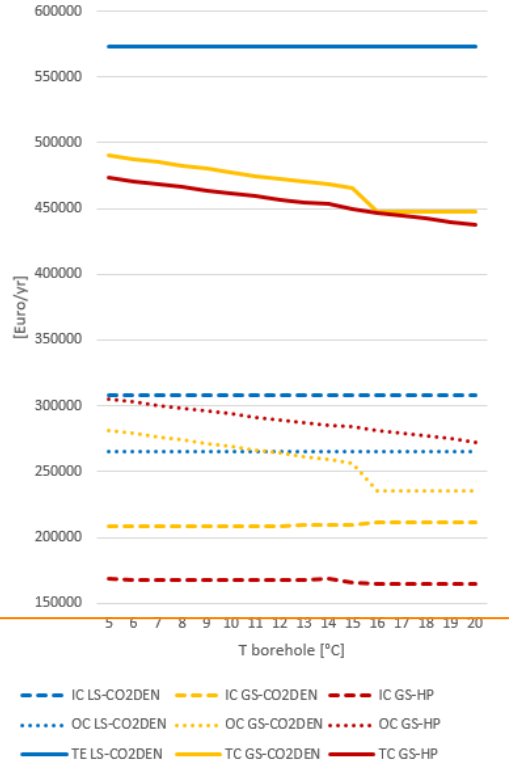
Assuming uniform soil and maintaining a constant heat capacity, a higher borehole temperature would imply drilling a smaller number of wells with greater depth. In other words, the geothermal model described in Section 3.2 simply models the heat capacity and the investment cost per meter well. It is thus not able to properly account for advanced correlations between heat capacity, cost function and well depth.

Nevertheless, this sensitivity analysis gives an idea of the global behavior response of the different conversion technologies to the ground temperature. This can be very helpful to estimate the performance of either system, in function of the geographical location, latitude and altitude.

## 5.4 Lake distance

As it has been seen in the previous paragraphs, the LS-CO2DEN presents competitive OC. Avoiding geothermal drilling can thus represent a big advantage, through the reduction of upfront costs. Pressure losses as well as the energy for pumping have been neglected, so the cost of the water pipes is mainly dependent on the distance of the lake water. Thus the threshold for the distance of the lake can be calculated, for which the LS-CO2DEN system to present a lower total cost than the GS-CO2DEN system.

This threshold temperature varies in function of the ground temperature, and it has been calculated accordingly. The resulting thresholds are plotted on Figure 34. This helps choosing between using the lake or the soil as a heat source, knowing the mean ground temperature and the distance from the lake water.



write and reference model with if conditions

Figure 33: Cost comparison of variants in function of the borehole temperature

wrapfig

At  $T_{borehole} = 12^\circ\text{C}$ , as in the Eglantine district, the LS-CO2DEN would be a financially interesting solution against GS-HP and GS-CO2DEN if the distance to the lake is respectively shorter than 328 and 484 meters.

### 5.5 External heat source

The integration of external heat sources, big as for example the ice rink in Eglantine case, is very interesting for this technology. However, this always depends on the ratio between the IC and the OC. In this case, this can be calculated with the ratio between the additional meters of pipes that have to be installed, wrt the amount of heat that can be recovered per year.

An new and efficient cooling system, together with an intelligent (weather, use, conditions...) management system, can drastically reduce energy consumption. This should be considered in the inclusion of the ice rink as heat source, since the renovation of the existing ice rink, or the construction of a new ice rink, would considerably reduce the amount of available waste heat.

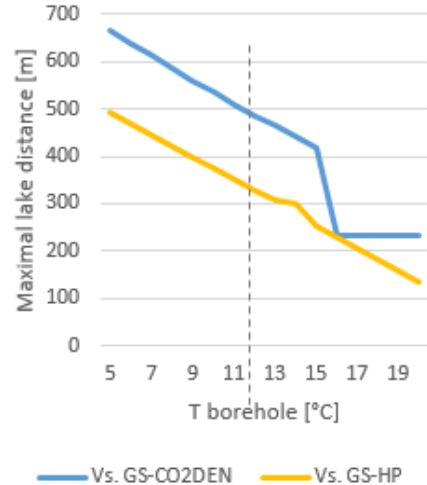


Figure 34: Maximum distance of lake for which the total costs are lower than the two other energy systems, in function of the ground temperature  $T_{borehole}$

good thing to do?

exergy and cop values

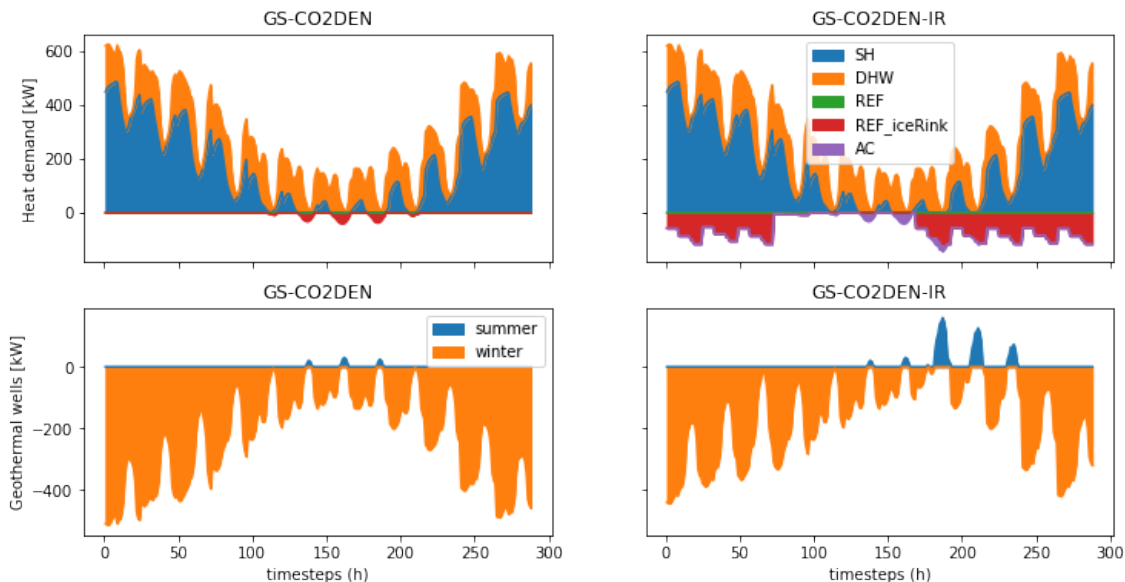


Figure 35: Heat supplied (above) and heat source use (below)

### 5.6 Optimization of energy demand

The Eglantine district is for 97% of residential use (see Section 4.1), resulting in a very low cooling and refrigeration demand. It is now legitimate to wonder how the different energy systems would perform in a different district, i.e. with a different building use and thus a differently composed energy demand. With this aim in mind, it is also interesting to find out the optimum district composition for the performance of a CO2DEN system.

As per Table 6, the building categories are:

1. Housing (Multidwelling)
2. Retail
3. Restaurant services
4. Indoor swimming pool

For sake of simplicity, among the categories shown in Table 6, the two most common and diverse - i.e. presenting the most different energy demand - have been chosen: (1) Housing and (2) Retail.

A sensitivity analysis has been performed on a district composed by those two categories. The energy demand resulting from the different combinations of the above mentioned categories is shown in Figure 36. It is clear to see that the Retail building has a high cooling demand during summer months, with demand peaks that are around 4 times the heating demand peaks. Moreover, while the space heating demand remains very similar, the hot water demand decreases considerably.

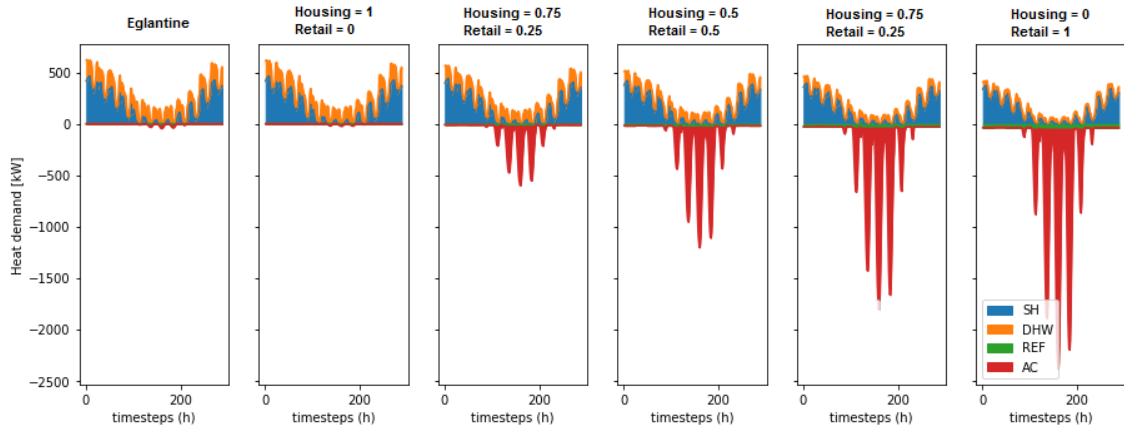


Figure 36: Comparison of the energy demand (power) for the different use of buildings throughout the year

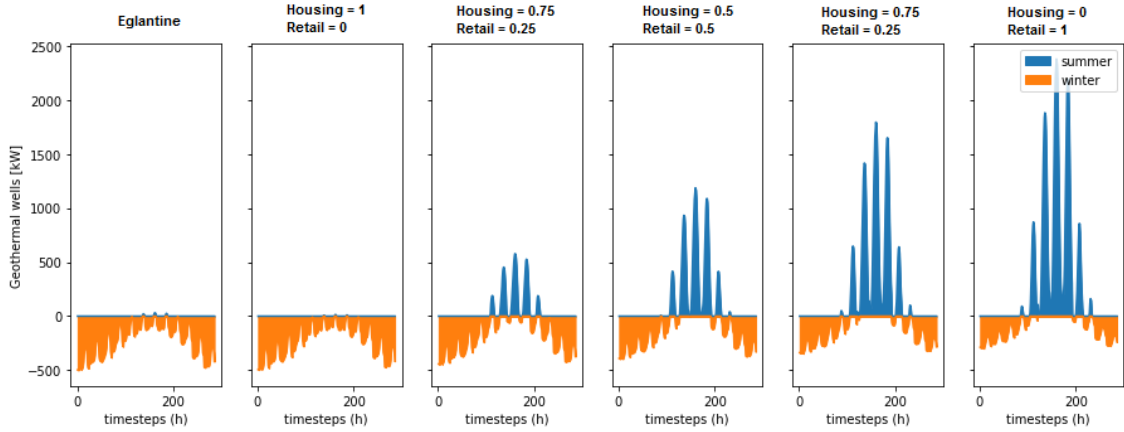


Figure 37: Comparison of the energy demand (power) of heat extracted (WINTER) of injected (SUMMER) into the boreholes

The resulting costs are shown in Figures 38.

Almost no difference in OC, Figure 38. There is no reason to lower OP since its about free cooling more than refrigeration. The only way if they happened in the same moment, since model does not account for heat storage in GTW.

needed  
figure of  
source?

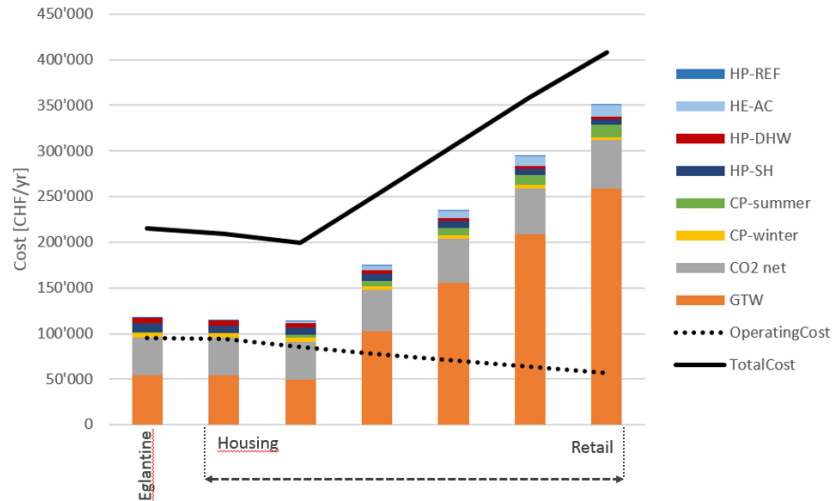


Figure 38: Cost comparison for different combinations of *housing* and *retail* building use, with the Eglantine district as a reference in the first column. The stacked columns show the investment costs.

The IC are strongly dependent on GTW cost. These are modeled in function of the peak demand. Thus given the very high cooling peaks originated by retail, the sizing of the gtw increases accordingly, what drastically increases the IC of the system.

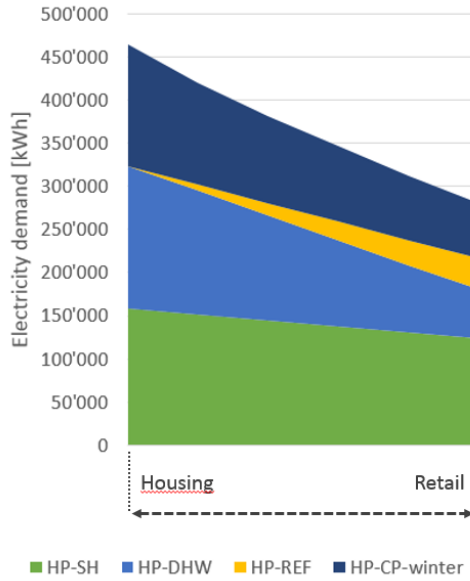


Figure 39: Electricity demand in function of the building use composition

But what is the optimum combination?

To answer this questions, a model has been implemented that lets the solver choose the composition of the district. This requires an additional set of constraints, which ensures that the chosen composition is maintained throughout all the timesteps:

$$f_{h,t} = f_{h,t+1} \quad \forall t \in T, h \in H \quad (79)$$

where  $f_{h,t}$  is the sizing variable of unit h in timestep t (see Section 2.6) and H is a subset of units U, corresponding to the above mentioned building categories.

Every unit h in H has been sized to the total ERA of the Eglantine district. Thus, in order to have comparable results, the next constraint ensures that the share of all h sum up to the size of the Eglantine district:

$$\sum_h^H f_{h,t} = 1 \quad \forall t \in T, h \in H \quad (80)$$

The combination presenting lowest total cost is found to be at:

$$f_{Retail} = 0.134$$

$$f_{Housing} = 0.866$$

### 5.6.1 Ground/CU

Now one could ask how this building use solution depends on Tground. Done a sensitivity analysis, with very interesting results.

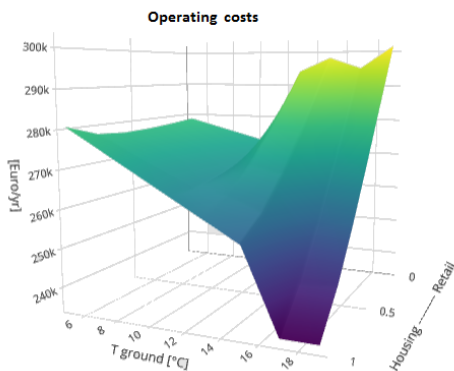


Figure 40: Operating costs in function of the borehole temperature and the building use in the district

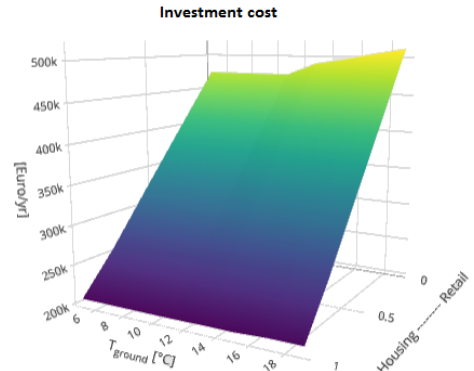


Figure 41: Investment costs in function of the borehole temperature and the building use in the district

Very interesting results, but again this shows that the cost model of GTW has to be optimized, since the difference seems to big.

## 6 Outlook

This and this has been analyzed and results have shown.

However, it would be very interesting to make detailed analysis of...

This model should be improved...

The crucial aspect are geothermal wells, its sizing and thus its investment costs. For this a better model should be developed.

Geothermal model: In Switzerland this would correspond to different well depth. To study this thoroughly it would be necessary to have a model for the geothermal well, taking into account the temperature gradient in function of depth, as well as the varying heat transfer coefficient for the CO2 vapor on the upward pipe[?, ?]. This model should also account for the recharge rate of the soil, which would improve the equipment sizing. And thus storage, or gain through restoring/injecting heat.

Conductivity models [?, ?, ?] This new thing could be integrated...

no storage technology has been taken into account. This would enable to adapt the consumption to profit from the cheap domestic produced energy. Definitely one of the next steps to improve the model!!!

## **7 Conclusion**

## References

## **8 Anergy nets Switzerland**

Table 20: District energy systems in Switzerland

	Anergiennetz ETH Hönggerberg	Jardins de la Pâla	Suurstoffi- Areal	Anergiennetz Friesenberg (FGZ)	CAD La- Tour-De-Peilz	Anergiennetz- Visp	Genève-Lac- Nations (GLN)
<b>Location</b>	Zürich	Bulle	Rotkreuz	Zürich	La-Tour-de-Peilz	Visp	Genève
<b>Year of construction</b>	2012 - 2026	2012 - 2020	2010 - 2020	2011-2050	2013 - 2015	2007 - heute	2008 - 2016
<b>Type</b>	i 20 °C	i 20 °C	i 20 °C	i 20 °C	i 20°C	i 20 °C	i 20 °C
<b>ERA [m<sup>2</sup>]</b>	475'000	65'000	172'421	185'000	24 Buildings	160'000	840'000
<b>Use</b>	School Residential	Residential Commercial Industry	Administration Commercial Catering School	Residential Computation	Residential Administration	Residential Industry	Residential Administration School
<b>Status</b>	Partly built	Partly built	Partly built	Partly built	Built	Built	Built
Data Energy Consumption							
<b>Inst. Heating capacity [kW]</b>	8'000	2'000	6'732	3'930	10'000	3'467	4'300
<b>Heating demand [MWh/a]</b>	28'450	3'100	10'619	35'000	812	8'737	5'000
<b>Inst. Cooling capacity [kW]</b>	6'000	1'000	2'327	3'500	None	2'600	16'200
<b>Cooling demand [MWh/a]</b>	26'200	650	2'364	80'000	None	3'380	20'000
<b>Heat source</b>	Laboratories waste heat +HP	Groundwater+HP	Waste heat buildings + PVT (solar th.) +HP	Waste heat data center+HP	Lake water +HP	Industrial waste heat + HP	Lake water +HP
<b>Heat storage</b>	Geothermal well field (431 at 200m)	Groundwater 12°C	Geothermal well field (215 at 150 m, 180 at 280m)	Geothermal well field (332 at 250m)	None	None	None
Network data							
<b>Network length [km]</b>	1.5	0.85	2.5	1.5	4.1	4.2	6
<b>Heating pipeT</b>	24 °C - 8 °C	12 °C - 9 °C	25 °C - 8 °C	28 °C - 8 °C	20 °C - 6 °C	18 °C - 8 °C	17 °C - 5 °C
<b>Cooling pipeT</b>	4 °C - 20 °C	4 °C - 17 °C	4 °C - 17 °C	4 °C -24 °C	2 °C - 16 °C	4 °C - 16 °C	5 °C - 12 °C
<b>Pipe diameter [mm]</b>	DN 560	75 - 250	60 - 400	400 - 500	400 -700	DN 400	100 -700
<b>Number of pipes</b>	3	2	2	2	2	2	2

Table 21: District energy systems in Switzerland

	Anergienetz ETH Hönggerberg	Jardins de la Pâla	Suurstoffi- Areal	Anergienetz Friesenberg (FGZ)	CAD La- Tour-De-Peilz	Anergienetz- Visp	Genève-Lac- Nations (GLN)
Financial data							
<b>Tot. investments '[Mio.CHF]'</b>	37	6	n/a	42.5	32	1.26	33
<b>Interest rate[%]</b>	3.9 - 6.7		n/a	n/a	6.4	5.8 - 8	n/a
<b>Lifespan [a]</b>							
Pipes	50	30	40	50	50	40	n/a
Storage	50	None	80	50	None	None	n/a
Heating unit	20	15	20	20	25	20	n/a
Cooling unit	20	15	20	20	25	20	n/a
<b>Cost of energy '[Rp./kWh]'</b>	7.7 (Heating +cooling)	5.85 – 8 (at the moment only heating)	n/a	18 (Heating)	19.8 (at the moment only heating)	22.9 (Heating + cooling)	n/a
<b>Tot. COP of heating</b>	7.2	4.4	n/a	5.2	n/a	n/a	n/a
<b>Tot. COP of heating (incl. Pumps...)</b>	5.8	2.7	2.7	4.1	3.5-4	4	6.5
<b>Tot. EER of cooling</b>	30.1	n/a	n/a	n/a	n/a	n/a	n/a
<b>Tot. EER of cooling (incl. Pumps...)</b>	6.9	12.1	n/a	n/a	n/a	n/a	n/a